PML and high-accuracy boundary integral equation solver for wave scattering by a locally defected periodic surface

Xiuchen Yu[1], Guanghui Hu[2], Wangtao Lu[3] and Andreas Rathsfeld[4]

August 3, 2021

Abstract

This paper studies the perfectly-matched-layer (PML) method for wave scattering in a half space of homogeneous medium bounded by a two-dimensional, perfectly conducting, and locally defected periodic surface, and develops a high-accuracy boundary-integral-equation (BIE) solver. Along the vertical direction, we place a PML to truncate the unbounded domain onto a strip and prove that the PML solution converges linearly to the true solution in the physical subregion of the strip with the PML thickness. Laterally, we divide the unbounded strip into three regions: a region containing the defect and two semi-waveguide regions, separated by two vertical line segments. In both semi-waveguides, we prove the well-posedness of an associated scattering problem so as to well define a Neumann-to-Dirichlet (NtD) operator on the associated vertical segment. The two NtD operators, serving as exact lateral boundary conditions, reformulate the unbounded strip problem as a boundary value problem onto the defected region. Due to the periodicity of the semi-waveguides, both NtD operators turn out to be closely related to a Neumann-marching operator, governed by a nonlinear Riccati equation. It is proved that the Neumann-marching operators are contracting, so that the PML solution decays exponentially fast along both lateral directions. The consequences culminate in two opposite aspects. Negatively, the PML solution cannot exponentially converge to the true solution in the whole physical region of the strip. Positively, from a numerical perspective, the Riccati equations can now be efficiently solved by a recursive doubling procedure and a high-accuracy PML-based BIE method so that the boundary value problem on the defected region can be solved efficiently and accurately. Numerical experiments demonstrate that the PML solution converges exponentially fast to the true solution in any compact subdomain of the strip.

1 Introduction

Due to its nearly reflectionless absorption of outgoing waves, perfectly matched layer or PML, since its invention by Berenger in 1994 [4], has become a primary truncation technique in a broad class of unbounded wave scattering problems [11, 31, 16], ranging from quantum mechanics, acoustics, electromagnetism (optics), to seismology. Mathematically,

[1]School of Mathematical Sciences, Zhejiang University, Hangzhou 310027, China. Email: yuxiuchen@zju.edu.cn.

[2]School of Mathematical Sciences, Nankai University, Tianjin 300071, China. Email: ghhu@nankai.edu.cn

[3]School of Mathematical Sciences, Zhejiang University, Hangzhou 310027, China. Email: wangtaolu@zju.edu.cn. This author is partially supported by NSF of Zhejiang Province for Distinguished Young Scholars (LR21A010001).

[4]Weierstrass Institute, Mohrenstr. 39, 10117 Berlin, Germany. Email: rathsfeld@wias-berlin.de

a PML can be equivalently understood as a complexified transformation of a coordinate [12]. A wave outgoing along the coordinate is then analytically continued in the complex plane and becomes exponentially decaying in the PML. However, it is such a double-edged feature that makes PML be placed only in the direction where the medium structure is invariant so as to guarantee the validity of analytic continuation. Consequently, PML loses its prominence for some complicated structures, such as periodic structures [20]. Motivated by this, this paper studies wave scattering in a half space of homogeneous medium bounded by a two-dimensional, perfectly conducting, and locally defected periodic surface, and investigate the potential of PML in designing an accurate boundary integral equation (BIE) solver for the scattering problem.

Let a cylindrical wave due to a line source, or a downgoing plane wave be specified above the defected surface. Then, a primary question is to understand clearly how the scattered wave radiates at infinity. Intrinsically, PML is highly related to the well-known Sommerfeld radiation condition (SRC), which, arguably, is an alternative way of saying "*wave is purely outgoing at infinity*". However, SRC is considered to be no longer valid for characterizing the scattered wave even when the surface is flat [2]. Instead, upward propagation radiation condition (UPRC), a.k.a angular spectrum representation condition [14] is commonly used, and can well pose the present problem or even more general rough surface scattering problems [5, 7, 8]. Milder than SRC, UPRC only requires that the scattered wave contain no downgoing waves on top of a straight line above the surface, allowing waves incoming horizontally from infinity.

If the surface has no defects, the total wave field for the plane-wave incidence is quasi-periodic so that the original scattering problem can be formulated in a single unit cell, bounded laterally but unbounded vertically. According to UPRC, the scattered wave at infinity can then be expressed in terms of upgoing Bloch waves, so that a transparent boundary condition or PML of a local/nonlocal boundary condition can be successfully used to terminate the unit cell vertically; readers are referred to [3, 10, 26, 34] and the references therein, for related numerical methods as well as theories of exponential convergence due to a PML truncation. But, if the incident wave is nonquasi-periodic, e.g., the cylindrical wave, or if the surface is locally defected, much fewer numerical methods or theories have been developed as it is no longer straightforward to laterally terminate the scattering domain. Existing laterally truncating techniques include recursive doubling procedure (RDP) [33, 15], Floquet-Bloch mode expansion [17, 19, 24], and Riccati - equation based exact boundary condition [21].

In a recent work [18], we proved that the total field for the cylindrical incidence, a.k.a the Green function, satisfies the standard SRC on top of a straight line above the surface. Based on this, we further revealed that for the plane-wave incidence, the perturbed part of the total field due to the defect satisfies the SRC as well. Consequently, this suggests to use a PML to terminate the vertical variable so as to truncate the unbounded domain to a strip, bounded vertically but unbounded laterally. In fact, such a natural setup of PML had already been adopted in the literature [33, 6, 32], without a rigorous justification of the outgoing behavior, though. It is worthwhile to mention that Chandler-Wilde and Monk in [6] rigorously proved that under a Neumann-condition PML, the PML solution converges to the true solution in the whole physical region of the strip at the rate of only algebraic order of PML thickness; they further revealed that the PML solution due to the cylindrical incidence for a flat surface decays exponentially at infinity of a rectangular strip. However, it remains unclear how the PML solution radiates at infinity of the more generally curved strip under consideration. On the other hand, no literally rigorous theory has been developed to clearly understand why this PML-truncated strip

2

can further be laterally truncated to a bounded domain by the aforementioned techniques without introducing artificial ill-posedness; in other words, the well-posedness of scattering problems in exterior regions of the truncated domain is unjustified.

To address these questions, we first prove in this paper that under a Dirichlet-condition PML, the PML solution due to the cylindrical incidence, i.e., Green's function of the strip, converges to the true solution in the physical subregion of the strip at an algebraic order of the PML thickness. Next, we split the strip into three regions: a bounded region containing the defect and two semi-waveguide regions of a single-directional periodic surface, separated by two vertical line segments. By use of Green's function of the strip, transparent boundary conditions can be developed to truncate the unbounded semi-waveguides. Based on this, we apply the method of variational formulation and Fredholm alternative to prove the well-posedness of the scattering problem in either semi-waveguide so as to define a Neumann-to-Dirichlet (NtD) operator on its associated vertical segment. The two NtD operators serve exactly as lateral boundary conditions to terminate the strip and to reformulate the unbounded strip problem as a boundary value problem on the defected region. Due to the periodicity of the semi-waveguides, both NtD operators turn out to be closely related to a Neumann-marching operator, which solves a nonlinear Riccatti equation. It is proved that the Neumann-marching operators are contracting, indicating that the PML solution decays exponentially fast along both lateral directions even for the curved strip. The consequences culminate in two opposite aspects. Positively, from a numerical perspective, the Riccati equations can be efficiently solved by an RDP method so that the strip can be laterally truncated with ease. Negatively, the PML solution shall never exponentially converge to the true solution in the whole physical region of the strip. Nevertheless, as conjectured in [6], exponential convergence is optimistically expected to be realizable in any compact subdomain of the strip.

To validate the above conjecture numerically, we employ a high-accuracy PML-based boundary integral equation (BIE) method [28] to execute the RDP so that the two Riccati equations can be accurately solved for the two Neumann-marching operators, respectively, and hence the two NtD operators terminating the strip can be obtained. With the two NtD operators well-prepared, the boundary value problem in the defected region can be accurately solved by the PML-based BIE method again. By carrying out several numerical experiments, we observe that the PML truncation error for wave field over the defected part of the surface decays exponentially fast as PML absorbing strength or thickness increases. This indicates that there is a chance that the PML solution still converges to the true solution exponentially in any compact subdomain of the strip, the justification of which remains open.

The rest of this paper is organized as follows. In section 2, we introduce the half-space scattering problem and present some known well-posedness results. In section 3, we introduce a Dirichlet-condition PML, prove the well-posedness of the PML-truncated problem and study the prior error estimate of the PML truncation. In section 4, we study well-posedness of the semi-waveguide problems. In section 5, we establish lateral boundary conditions, prove the exponentially decaying property of the PML solution at infinity of the strip, and develop an RDP technique to get the lateral boundary conditions. In section 6, we present a PML-based BIE method to numerically solve the scattering problem. In section 7, numerical experiments are carried out to demonstrate the performance of the proposed numerical method and to validate the proposed theory. We draw our conclusion finally in section 8 and propose some future plans.

2 Problem formulation

Let $\Omega \times \mathbb{R} \subset \mathbb{R}^3$ be an x_3-invariant domain bounded by a perfectly-conducting surface $\Gamma \times \mathbb{R}$, where $\Gamma \subset \mathbb{R}^2$, bounding domain $\Omega \subset \mathbb{R}^2$, is a local perturbation of a T-periodic curve $\Gamma_T \subset \mathbb{R}^2$ periodic in x_1-direction, as shown in Figure 1(a). We denote the Cartesian
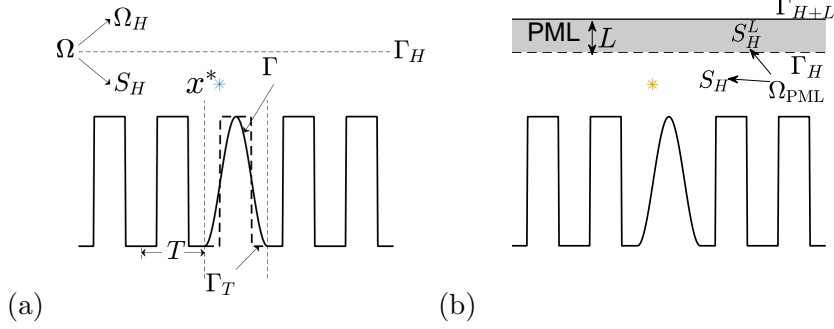
Figure 1: (a) A sketch of the half-space scattering problem. (b) A PML placed above Γ. The scattering surface Γ locally perturbs the periodic curve Γ_T of period T. x^* represents the exciting source. Γ_H is an artificial interface, on which a DtN map is defined or a PML is placed.

coordinate system of $\mathbb{R}^3$ by (x_1, x_2, x_3) and let $x = (x_1, x_2) \in \Omega$. Throughout this paper, we shall assume that Γ is Lipschitz and that Ω satisfies the following geometrical condition

$$(\text{GC1}): \quad (x_1, x_2) \in \Omega \Rightarrow (x_1, x_2 + a) \in \Omega, \quad \forall a \geq 0.$$

For simplicity, suppose Γ only perturbs one periodic part of Γ_T, say $|x_1| < \frac{T}{2}$.

Let the unbounded domain $\Omega \times \mathbb{R}$ be filled by a homogeneous medium of refractive index n. For a time-harmonic transverse-electric (TE) polarized electro-magnetic wave, of time dependence $e^{-\mathbf{i}\omega t}$ for the angular frequency ω, the x_3-component of the electric field, denoted by u^{tot}, is x_3-invariant and satisfies the following two-dimensional (2D) Helmholtz equation

$$\Delta u^{\text{tot}} + k^2 u^{\text{tot}} = 0, \quad \text{on} \quad \Omega, \tag{1}$$

$$u^{\text{tot}} = 0, \quad \text{on} \quad \Gamma, \tag{2}$$

where $\Delta = \partial_{x_1}^2 + \partial_{x_2}^2$ is the 2D Laplacian and $k = k_0 n$ with $k_0 = \frac{2\pi}{\lambda}$ denoting the free-space wavenumber for wavelength λ.

Let an incident wave u^{inc} be specified in Ω and let $x = (x_1, x_2) \in \Omega$. In this paper, we shall mainly focus on the following two cases of incidences: (i) a plane wave $u^{\text{inc}}(x) = e^{\mathbf{i}k(\cos\theta x_1 - \sin\theta x_2)}$ for the incident angle $\theta \in (0, \pi)$; (ii) a cylindrical wave $u^{\text{inc}}(x; x^*) = G(x; x^*) = \frac{\mathbf{i}}{4} H_0^{(1)}(k|x - x^*|)$ excited by a source at $x^* = (x_1^*, x_2^*) \in \Omega$. In the latter case, equation (1) should be replaced by

$$\Delta u^{\text{tot}} + k^2 u^{\text{tot}} = -\delta(x - x^*), \tag{3}$$

so that $u^{\text{tot}}(x; x^*)$ in fact represents the Green function excited by the source point x^*. For simplicity, we assume that $|x_1^*| < T/2$ so that x^* is right above the perturbed part of Γ.

Let $u^{\text{sc}} = u^{\text{tot}} - u^{\text{inc}}$ denote the scattered wave. One may enforce the following UPRC:

$$u^{\text{sc}}(x) = 2 \int_{\Gamma_H} \frac{\partial G(x; y)}{\partial y_2} u^{\text{sc}}(y) ds(y), \tag{4}$$

4

where $\Gamma_H = \{(x_1, H) : x_1 \in \mathbb{R}\}$ denotes a straight line strictly above Γ for some $H > 0$ and $y = (y_1, y_2)$. According to [7], the UPRC helps to define a Dirichlet-to-Neumann map $\mathcal{T} : H^{1/2}(\Gamma_H) \to H^{-1/2}(\Gamma_H)$ for the domain $\Omega_H = \{x \in \Omega : x_2 > H\}$, such that for any $\phi \in H^{1/2}(\Gamma_H)$,

$$\mathcal{T}\phi = \mathcal{F}^{-1} M_z \hat{\phi}, \tag{5}$$

where $\hat{\phi}(H; \xi) = [\mathcal{F}\phi](H; \xi)$ denotes the following normalized Fourier transform

$$[\mathcal{F}\phi](H; \xi) = \frac{1}{\sqrt{2\pi}} \int_{\mathbb{R}} \phi(x_1, H) e^{-\mathbf{i}\xi x_1} dx_1, \tag{6}$$

and the operator M_z in the space of Fourier transforms is the operator of multiplication by

$$z(\xi) = \begin{cases} -\mathbf{i}\sqrt{k^2 - \xi^2}, & \text{for } |\xi| \leq k, \\ \sqrt{\xi^2 - k^2}, & \text{for } |\xi| > k. \end{cases} \tag{7}$$

Then, we may enforce

$$\partial_\nu u^{\text{sc}} = -\mathcal{T}u^{\text{sc}}, \quad \text{on} \quad \Gamma_H, \tag{8}$$

where, unless otherwise indicated, ν always denotes the outer unit normal vector on Γ_H. The UPRC guarantees the well-posedness of our scattering problem [7], but allows u^{sc} containing incoming waves, largely limiting its applications in designing numerical algorithms. Nevertheless, our recent work [18] has shown a stronger Sommerfeld-type condition for the aforementioned two incidences, which still preserves the well-posedness. Note that [18] assumes further the following condition:

(GC2): some (and hence any) period of Γ_T contains a line segment,

which guarantees a local behavior of the Green function $u^{\text{tot}}(x; y)$ for any x, y sufficiently close to each line segment. Let $S_H = \Omega \cap \{x : x_2 < H\}$ be the strip between Γ_H and Γ. The radiation condition reads as follows:

(i). For the plane-wave incidence, $u^{\text{og}} := u^{\text{tot}} - u^{\text{tot}}_{\text{ref}}$, where $u^{\text{tot}}_{\text{ref}}$ is the reference scattered field for the unperturbed scattering curve $\Gamma = \Gamma_T$, satisfies the following half-plane Sommerfeld radiation condition (hSRC): for some sufficiently large $R > 0$ and any $\rho < 0$,

$$\lim_{r \to \infty} \sup_{\alpha \in [0,\pi]} \sqrt{r} |\partial_r u^{\text{og}}(x) - \mathbf{i}k u^{\text{og}}(x)| = 0, \sup_{r \geq R} r^{1/2} |u^{\text{og}}(x)| < \infty, \text{ and } u^{\text{og}} \in H^1_\rho(S_H^R), \tag{9}$$

where $x = (r\cos\alpha, H + r\sin\alpha)$, $S_H^R = S_H \cap \{x : |x_1| > R\}$, and $H^1_\rho(\cdot) = (1 + x_1^2)^{-\rho/2} H^1(\cdot)$ denotes a weighted Sobolev space. We defer the computation of $u^{\text{tot}}_{\text{ref}}$ to section 6.3.

(ii). For the cylindrical incidence, the total field $u^{\text{og}} := u^{\text{tot}}$ itself satisfies the hSRC (9) in Ω_H. Thus, the scattered field u^{sc} satisfies (9) as well since u^{inc} satisfies (9).

Certainly, u^{og} satisfies the UPRC condition (4) such that (8) holds for u^{og} in place of u^{sc} [9, Them. 2.9(ii)]. In the following, we shall consider the cylindrical incidence only and the plane-wave incidence case can be analyzed similarly.

We recall some important results from [7]. To remove the singularity of the right-hand side of (3), let

$$u^{\text{og}}_r(x; x^*) = u^{\text{og}}(x; x^*) - \chi(x; x^*)u^{\text{inc}}(x; x^*), \tag{10}$$

where the cut-off function $\chi(x; x^*) = 1$ in a neighborhood of x^* and has a sufficiently small support enclosing x^*. Let $V_H = \{\phi|_{S_H} : \phi \in H_0^1(\Omega)\}$. Then, it is equivalent to seek $u_r^{\mathrm{og}} \in V_H$ that satisfies the following boundary value problem

$$\Delta u_r^{\mathrm{og}} + k^2 u_r^{\mathrm{og}} = g, \quad \text{on} \quad S_H, \tag{11}$$

$$\partial_\nu u_r^{\mathrm{og}} = -\mathcal{T} u_r^{\mathrm{og}}, \quad \text{on} \quad \Gamma_H, \tag{12}$$

where $g = -[\Delta \chi]u^{\mathrm{inc}} - 2\sum_{j=1}^2 \partial_{x_j}\chi \partial_{x_j} u^{\mathrm{inc}} \in L^2(S_H)$ such that supp g is in the neighborhood of x^* contained in $\overline{S_H}$. An equivalent variational formulation reads as follows: Find $u_r^{\mathrm{og}} \in V_H$, such that for any $\phi \in V_H$,

$$b(u_r^{\mathrm{og}}, \phi) = -(g, \phi)_{S_H}, \tag{13}$$

where the sesqui-linear form $b(\cdot, \cdot) : V_H \times V_H \to \mathbb{C}$ is given by

$$b(\phi, \psi) = \int_{S_H} (\nabla \phi \cdot \nabla \bar{\psi} - k^2 \phi \bar{\psi}) dx + \int_{\Gamma_H} \mathcal{T} \phi \bar{\psi} ds. \tag{14}$$

It has been shown in [7] that b satisfies the following inf-sup condition: for all $v \in V_H$,

$$\gamma ||v||_{V_H} \leq \sup_{\phi \in V_H} \frac{|b(v, \phi)|}{||\phi||_{V_H}}, \tag{15}$$

where $\gamma > 0$ depends on H, k and Ω. Furthermore, b defines an invertible operator $\mathcal{A} : V_H \to V_H^*$ such that $(\mathcal{A}\phi, \psi) = b(\phi, \psi)$ and $||\mathcal{A}^{-1}|| \leq \gamma^{-1}$. Thus, $u_r^{\mathrm{og}} = -\mathcal{A}^{-1}g$ so that $u^{\mathrm{og}} = -\mathcal{A}^{-1}g + \chi u^{\mathrm{inc}}$.

The hSRC (9) suggests to compute the outgoing wave u^{og} numerically, as the PML technique[4, 6] could apply now to truncate the x_2-direction. In the following sections, we shall first introduce the setup of a PML to truncate x_2 and then develop an accurate lateral boundary condition to truncate x_1.

3 PML Truncation

Mathematically, the PML truncating x_2 introduces a complexified coordinate transformation

$$\tilde{x}_2 = x_2 + \mathbf{i}S \int_0^{x_2} \sigma(t) dt, \tag{16}$$

where $\sigma(x_2) = 0$ for $x_2 \leq H$ and $\sigma(x_2) \geq 0$ for $x_2 \geq H$; note that such a tilde notation can also be used to define $\tilde{y}_2$ and $\tilde{x}_2^*$ in the following. As shown in Figure 1(b), the planar strip $S_H^L = \mathbb{R} \times [H, H + L]$ with nonzero σ is called the PML region so that L represents its thickness. In this paper, we choose an $m \geq 0$ and,

$$\sigma(x_2) = \begin{cases} \frac{2f_2^m}{f_1^m + f_2^m}, & x_2 \in [H, H + L/2] \\ 2, & x_2 \geq H + L/2, m \neq 0 \\ 1, & x_2 \geq H + L/2, m = 0 \end{cases} \tag{17}$$

where we note that $\sigma \equiv 1$ if $m = 0$, and

$$f_1 = \left(\frac{1}{2} - \frac{1}{m}\right)\xi^3 + \frac{\xi}{m} + \frac{1}{2}, \quad f_2 = 1 - f_1, \quad \xi = \frac{2x_2 - (2H + L/2)}{L/2}.$$

Let $L_c := \tilde{x}_2(H+L) - H = L + \mathbf{i}S_c L$, where $S_c = \frac{S}{L}\int_H^{H+L}\sigma(t)dt$. Both the real part and imaginary part of L_c affect the absorbing strength of the PML [12].

Now, let $\tilde{x} = (x_1, \tilde{x}_2)$. For $x^* \in S_H$, according to (4), we can define by analytic continuation that

$$u^{\text{og}}(\tilde{x};x^*) := 2\int_{\Gamma_H}\frac{\partial G(\tilde{x};y)}{\partial y_2}u^{\text{og}}(y;x^*)ds(y),$$

that satisfies

$$\tilde{\Delta}u^{\text{og}}(\tilde{x};x^*) + k^2 u^{\text{og}}(\tilde{x};x^*) = -\delta(x-x^*),$$

where $\tilde{\Delta} = \partial_{x_1}^2 + \partial_{\tilde{x}_2}^2$. By chain rules, we see that $\tilde{u}^{\text{og}}(x;x^*) := u^{\text{og}}(\tilde{x};x^*)$ satisfies

$$\nabla\cdot(\mathbf{A}\nabla\tilde{u}^{\text{og}}) + k^2\alpha\tilde{u}^{\text{og}} = -\delta(x-x^*), \quad \text{on } \Omega_{\text{PML}}, \tag{18}$$

$$\tilde{u}^{\text{og}} = 0, \quad \text{on } \Gamma. \tag{19}$$

where $\mathbf{A} = \text{diag}\{\alpha(x_2), 1/\alpha(x_2))\}$, $\alpha(x_2) = 1 + \mathbf{i}S\sigma(x_2)$, and the PML region $\Omega_{\text{PML}} = \Omega\cap\{x:x_2\le H+L\}$ consists of the physical region S_H and the PML region S_H^L. On the PML boundary $x_2 = H+L$, we use the homogeneous Dirichlet boundary condition

$$\tilde{u}^{\text{og}} = 0, \quad \text{on } \Gamma_{H+L} = \{x:x_2 = H+L\}. \tag{20}$$

The authors in [6] adopted a Neumann condition on the PML boundary Γ_{H+L} and proved the well-posedness of the related PML truncation problem. Here, we choose the Dirichlet condition (20) since, as we shall see, our numerical results indicate that the Dirichlet-PML seems more stable than the Neumann-PML. Furthermore, we need Green's function of the strip $\tilde{u}^{\text{og}}(x;x^*)$ for any $x^*\in\Omega_{\text{PML}}$ but not limited to S_H to establish lateral boundary conditions. For completeness, we shall, following the idea of [6], study the well-posedness of the problem (18-20) for any $x^*\in\Omega_{\text{PML}}$.

The fundamental solution of the anisotropic Helmholtz equation (18) is [28]

$$\tilde{G}(x;y) = G(\tilde{x};\tilde{y}) = \frac{\mathbf{i}}{4}H_0^{(1)}[k\rho(\tilde{x};\tilde{y})], \tag{21}$$

where $\tilde{y} = (y_1, \tilde{y}_2)$, the complexified distance function ρ is defined to be

$$\rho(\tilde{x},\tilde{y}) = [(x_1-y_1)^2 + (\tilde{x}_2-\tilde{y}_2)^2]^{1/2}, \tag{22}$$

and the half-power operator $z^{1/2}$ is chosen to be the branch of $\sqrt{z}$ with nonnegative real part for $z\in\mathbb{C}\backslash(-\infty,0]$ such that $\arg(z^{1/2})\in[0,\pi)$. The special choice of σ in (17) ensures that

$$\tilde{G}(x;y) = \tilde{G}(x;y_{\text{imag}}), \tag{23}$$

for any $x\in\Gamma_{H+L}$, when $y = (y_1,y_2)$ and $y_{\text{imag}} = (y_1, 2(H+L)-y_2)$, the mirror image of y w.r.t line Γ_{H+L}, are sufficiently close to Γ_{H+L} so that $\rho(\tilde{x};\tilde{y}) = \rho(\tilde{x};\tilde{y}_{\text{imag}})$.

To remove the singularity of the right-hand side of (18), we introduce

$$\tilde{u}_r^{\text{og}}(x;x^*) = \tilde{u}^{\text{og}}(x;x^*) - \chi(x;x^*)\tilde{u}^{\text{inc}}(x;x^*), \tag{24}$$

with the same cut-off function χ as in (10), where $\tilde{u}^{\text{inc}}(x;x^*) = u^{\text{inc}}(\tilde{x};\tilde{x}^*)$. Then, $\tilde{u}_r^{\text{og}}$ satisfies

$$\nabla\cdot(\mathbf{A}\nabla\tilde{u}_r^{\text{og}}) + k^2\alpha\tilde{u}_r^{\text{og}} = \tilde{g}^{\text{inc}}, \quad \text{on } \Omega_{\text{PML}}, \tag{25}$$

$$\tilde{u}_r^{\text{og}} = 0, \quad \text{on } \Gamma, \tag{26}$$

$$\tilde{u}_r^{\text{og}} = 0, \quad \text{on } \Gamma_{H+L}, \tag{27}$$

where $\tilde{g}^{\text{inc}} = [\nabla \cdot (\mathbf{A}\nabla) + k^2\alpha](1 - \chi(x; x^*))\tilde{u}^{\text{inc}}(x; x^*) \in L^2(\Omega_{\text{PML}})$ with $\text{supp } \tilde{g}^{\text{inc}} \subset \overline{\Omega_{\text{PML}}} = \overline{S_H} \cup \overline{S_H^L}$. Considering that x^* can be situated in S_H^L, $\text{supp } \tilde{g}^{\text{inc}}$ may not completely lie in the physical domain S_H. To establish a Dirichlet-to-Neumann map on Γ_H like (8), we need to study the following boundary value problem in the PML strip S_H^L: given $q \in H^{1/2}(\Gamma_H)$, $s \in H^{1/2}(\Gamma_{H+L})$, and $\tilde{g}^{\text{inc}}_{\text{PML}} = \tilde{g}^{\text{inc}}|_{S_H^L} \in L^2(S_H^L)$ with $\text{supp } \tilde{g}^{\text{inc}}_{\text{PML}} \subset \overline{S_H^L}$, find $v \in H^1(S_H^L)$ such that

$$\nabla \cdot (\mathbf{A}\nabla v) + k^2\alpha v = \tilde{g}^{\text{inc}}_{\text{PML}}, \quad \text{on} \quad S_H^L, \tag{28}$$

$$v = q, \quad \text{on} \quad \Gamma_H, \tag{29}$$

$$v = s, \quad \text{on} \quad \Gamma_{H+L}. \tag{30}$$

Let

$$v_0(x) = v(x) - \int_{S_H^L}[\tilde{G}(x; y) - \tilde{G}(x; y_{\text{imag}})]\tilde{g}^{\text{inc}}_{\text{PML}}(y)dy := v(x) - v^{\text{inc}}_{\text{PML}}(x),$$

where we recall that y_{imag} is the mirror image of y w.r.t line Γ_{L+H}. Thus, v_0 satisfies

$$\nabla \cdot (\mathbf{A}\nabla v_0) + k^2\alpha v_0 = 0, \quad \text{on} \quad S_H^L, \tag{31}$$

$$v_0 = q_n, \quad \text{on} \quad \Gamma_H, \tag{32}$$

$$v_0 = s_n, \quad \text{on} \quad \Gamma_{H+L}, \tag{33}$$

where $q_n = q - v^{\text{inc}}_{\text{PML}}|_{\Gamma_H} \in H^{1/2}(\Gamma_H)$ and $s_n = s - v^{\text{inc}}_{\text{PML}}|_{\Gamma_{H+L}} \in H^{1/2}(\Gamma_{H+L})$.

Looking for v_0 in terms of only complexified plane waves, we get

$$\hat{v}_0(x_2; \xi) = [\mathcal{F}v_0](x_2; \xi) = A\exp(z(\xi)(\tilde{x}_2 - H)) + B\exp(-z(\xi)(\tilde{x}_2 - H)), \tag{34}$$

where we recall that z has been defined in (7),

$$A(\xi) = \frac{\hat{s}_n(\xi) - \exp(-z(\xi)L_c)\hat{q}_n(\xi)}{\exp(z(\xi)L_c) - \exp(-z(\xi)L_c)}, \quad \text{and} \quad B(\xi) = \frac{-\hat{s}_n(\xi) + \exp(z(\xi)L_c)\hat{q}_n(\xi)}{\exp(z(\xi)L_c) - \exp(-z(\xi)L_c)},$$

$\hat{s}_n(\xi) = [\mathcal{F}s_n](H + L; \xi)$ and $\hat{q}_n(\xi) = [\mathcal{F}q_n](H; \xi)$. Here, to make A and B well-defined, we could let ξ travel through a Sommerfeld integral path $-\infty + 0\mathbf{i} \to 0 \to \infty - 0\mathbf{i}$ instead of $\mathbb{R}$ [25] such that $z \neq 0$. Consequently,

$$-\frac{\partial \hat{v}_0}{\partial x_2}\Big|_{x_2=H} = z\frac{-2}{\exp(zL_c) - \exp(-zL_c)}\hat{s}_n + z\frac{\exp(zL_c) + \exp(-zL_c)}{\exp(zL_c) - \exp(-zL_c)}\hat{q}_n. \tag{35}$$

Now define two bounded operators $\mathcal{T}_p : H^{1/2}(\Gamma_H) \to H^{-1/2}(\Gamma_H)$ by

$$\mathcal{F}[\mathcal{T}_p q_n](H; \xi) = z\frac{\exp(zL_c) + \exp(-zL_c)}{\exp(zL_c) - \exp(-zL_c)}\hat{q}_n,$$

and $\mathcal{N}_p : H^{1/2}(\Gamma_{H+L}) \to H^{-1/2}(\Gamma_H)$ by

$$\mathcal{F}[\mathcal{N}_p s_n](H + L; \xi) = z\frac{-2}{\exp(zL_c) - \exp(-zL_c)}\hat{s}_n;$$

note that the above definitions allow $\xi \in \mathbb{R}$ now, since limits can be considered when $z = 0$. Returning back to the PML-truncated problem (25-27), we reformulate it as an equivalent boundary value problem on the physical region S_H: Find $\tilde{u}^{\text{og}}_r \in V_H$ that satisfies

$$\nabla \cdot (\mathbf{A}\nabla \tilde{u}^{\text{og}}_r) + k^2\alpha \tilde{u}^{\text{og}}_r = \tilde{g}^{\text{inc}}|_{S_H}, \quad \text{on} \quad S_H, \tag{36}$$

8

$$\partial_\nu \tilde{u}_r^{\mathrm{og}} = -\mathcal{T}_p \tilde{u}_r^{\mathrm{og}}|_{\Gamma_H} + f_p, \quad \text{on} \quad \Gamma_H, \tag{37}$$

where

$$f_p = \mathcal{N}_p(v_{\mathrm{PML}}^{\mathrm{inc}}|_{\Gamma_{H+L}}) + \mathcal{T}_p(v_{\mathrm{PML}}^{\mathrm{inc}}|_{\Gamma_H}) + \partial_\nu v_{\mathrm{PML}}^{\mathrm{inc}}|_{\Gamma_H} \in H^{-1/2}(\Gamma_H). \tag{38}$$

The associated variational formulation reads as follows: Find $\tilde{u}_r^{\mathrm{og}} \in V_H$, such that for any $\psi \in V_H$,

$$b_p(\tilde{u}_r^{\mathrm{og}}, \psi) = -\int_{S_H} \tilde{g}^{\mathrm{inc}}|_{S_H} \bar{\psi} dx + \int_{\Gamma_H} f_p \bar{\psi} ds, \tag{39}$$

where the sesquilinear form $b_p(\cdot, \cdot) : V_H \times V_H \to \mathbb{C}$ is given by

$$b_p(\phi, \psi) = \int_{S_H} (\nabla \phi \cdot \nabla \bar{\psi} - k^2 \phi \bar{\psi}) dx + \int_{\Gamma_H} \bar{\psi} \mathcal{T}_p \phi ds. \tag{40}$$

As in [6], we define the following k-dependent norm

$$||\phi||_{H^s(\mathbb{R})}^2 = \int_{\mathbb{R}} (k^2 + \xi^2)^s |[\mathcal{F}\phi](\xi)|^2 d\xi$$

for $H^s(\mathbb{R})$. Then, the following lemma characterizes a rough difference of $\mathcal{T}_p$ away from $\mathcal{T}$.

Lemma 3.1 *We have for any $kS_cL > 0$,*

$$||\mathcal{T} - \mathcal{T}_p|| \leq \frac{1}{kS_cL}. \tag{41}$$

Proof 1 *By a simple analysis, it can be seen that*

$$\begin{aligned}
||\mathcal{T} - \mathcal{T}_p|| &= \sup_{\xi \in \mathbb{R}} \frac{|z(\xi)|}{\sqrt{k^2 + \xi^2}} |1 - \coth(z(\xi)L_c)| \\
&= \sup_{\xi \in \mathbb{R}} \frac{2|z(\xi) \exp(-2z(\xi)L_c)|}{\sqrt{k^2 + \xi^2}|1 - \exp(-2z(\xi)L_c)|} = \max\{S_1, S_2\},
\end{aligned}$$

where we recall that $L_c = L + \mathbf{i}S_cL$,

$$\begin{aligned}
S_1 &= \sup_{0 \leq t \leq 1} \frac{2t \exp(-2tkS_cL)}{\sqrt{2 - t^2}\sqrt{1 + \exp(-4tkL) - 2\cos(2tkS_cL)\exp(-2tkL)}} \\
&= \sup_{0 \leq t \leq 1} \frac{2t \exp(-2tkS_cL)}{\sqrt{2 - t^2}\sqrt{(1 - \exp(-2tkL))^2 + 4\exp(-2tkL)\sin^2(tkS_cL)}}
\end{aligned}$$

and

$$S_2 = \sup_{t \geq 1} \frac{2t \exp(-2tkS_cL)}{\sqrt{2 + t^2}\sqrt{(1 - \exp(-2tkL))^2 + 4\exp(-2tkL)\sin^2(tkS_cL)}}.$$

Clearly, $S_2 \leq 2\exp(-2kL)$. Since for $t \geq 0$,

$$f(t) = \frac{t \exp(-2tkS_cL)}{1 - \exp(-2tkS_cL)}$$

is nonincreasing, it is easy to see that $S_1 \leq 2f(0) = \frac{1}{kS_cL}$.

We do not intend to study the relation of $||\mathcal{T}_p - \mathcal{T}||$ and the other parameter S_c, as was done in [6] to optimize the performance of the PML, since the estimate in Lemma 3.1 is enough. Clearly, the sesquilinear form b_p in (40) defines a bounded linear functional $\mathcal{A}_p : V_H \to V_H^*$ such that: for any $\phi \in V_H$,

$$((\mathcal{A} - \mathcal{A}_p)\phi, \psi) = b(\phi, \psi) - b_p(\phi, \psi) = \int_{\Gamma_H} \bar{\psi}(\mathcal{T} - \mathcal{T}_p)\phi ds.$$

Analogous to [6, Sec. 3], we see immediately that

$$||\mathcal{A} - \mathcal{A}_p|| \leq 2||\mathcal{T} - \mathcal{T}_p|| \leq \frac{2}{kS_cL}.$$

Consequently, $\mathcal{A}_p$ has a bounded inverse provided that S_cL is sufficiently large as $\mathcal{A}$ is invertible. Since the right-hand side of (39) defines a bounded functional in V_H^*, we in fact have justified the following well-posedness result.

Theorem 3.1 *Provided that S_cL is sufficiently large, the PML-truncated problem (18), (19) and (20) admits a unique solution $\tilde{u}^{\mathrm{og}}(x; x^*) = \tilde{u}_r^{\mathrm{og}}(x; x^*) + \chi(x; x^*)\tilde{u}^{\mathrm{inc}}(x; x^*)$ with $\tilde{u}_r^{\mathrm{og}} \in H_0^1(\Omega_{\mathrm{PML}}) = \{\phi \in H^1(\Omega_{\mathrm{PML}}) : \phi|_{\Gamma \cup \Gamma_{H+L}} = 0\}$ for any $x^* \in \Omega_{\mathrm{PML}}$ such that $||\tilde{u}_r^{\mathrm{og}}(\cdot; x^*)||_{H^1(\Omega_{\mathrm{PML}})} \leq C||\tilde{g}^{\mathrm{inc}}||_{L^2(\Omega_{\mathrm{PML}})}$.*

Remark 3.1 *The well-posedness in Theorem 3.1 holds in general for any Lipschitz curve satisfying (GC1).*

Since for any $\phi \in V_H$,

$$b_p(\phi, \psi) = b(\phi, \psi) - \int_{\Gamma_H} \bar{\psi}(\mathcal{T} - \mathcal{T}_p)\phi ds,$$

the inf-sup condition (15) of b implies the inf-sup condition of b_p: for any $\phi \in V_H$,

$$\sup_{\psi \in V_H} \frac{|b_p(\phi, \psi)|}{||\psi||_{V_H}} \geq \sup_{\psi \in V_H} \frac{|b(\phi, \psi)|}{||\psi||_{V_H}} - \frac{2}{kS_cL}||\phi||_{V_H} \geq (\gamma - \frac{2}{kS_cL})||\phi||_{V_H}, \qquad (42)$$

provided S_cL is sufficiently large. As a consequence of (42), we immediately obtain the prior error estimate for the PML truncation if $x^* \in S_H$.

Corollary 3.1 *Provided that S_cL is sufficiently large,*

$$||u^{\mathrm{og}}(\cdot; x^*) - \tilde{u}^{\mathrm{og}}(\cdot; x^*)||_{V_H} \leq \frac{2}{\gamma kS_cL - 2}||u_r^{\mathrm{og}}(\cdot; x^*)||_{V_H}. \qquad (43)$$

whenever $x^* \in S_H$.

Proof 2 *Since for $x^* \in S_H$, $(u^{\mathrm{og}} - \tilde{u}^{\mathrm{og}})|_{S_H} = (u_r^{\mathrm{og}} - \tilde{u}_r^{\mathrm{og}})|_{S_H} \in V_H$, we have for any $\phi \in V_H$,*

$$b_p(u_r^{\mathrm{og}} - \tilde{u}_r^{\mathrm{og}}, \phi) = -\int_{\Gamma_H} \bar{\phi}(\mathcal{T} - \mathcal{T}_p)u_r^{\mathrm{og}} ds,$$

so that by the inf-sup condition (42),

$$||u_r^{\mathrm{og}} - \tilde{u}_r^{\mathrm{og}}||_{V_H} \leq (\gamma - \frac{2}{kS_cL})^{-1} \sup_{\phi \in V_H} \frac{|b_p(u_r^{\mathrm{og}} - \tilde{u}_r^{\mathrm{og}}, \phi)|}{||\phi||_{V_H}} = (\gamma - \frac{2}{kS_cL})^{-1} \sup_{\phi \in V_H} \frac{|\int_{\Gamma_H} \bar{\phi}(\mathcal{T} - \mathcal{T}_p)u_r^{\mathrm{og}} ds|}{||\phi||_{V_H}}$$

$$\leq \frac{2}{(\gamma - \frac{2}{kS_cL})kS_cL}||u_r^{\mathrm{og}}||_{V_H}.$$

10

4 Semi-waveguide problems

Unlike the exponential convergence results in [10, 34], (43) indicates only a poor convergence of the PML method over S_H. We however believe that exponential convergence can be realized in a compact subset of S_H, which is indeed true if Γ is flat [6]. This leads to an essential question after the vertical PML truncation: how to accurately truncate Ω_{PML} in the lateral x_1-direction? To address this question, as inspired by [21] and as illustrated in Figure 2 (a), we shall consider the following two semi-waveguide problems:

$$
(P^\pm): \quad
\begin{cases}
\nabla \cdot (\mathbf{A}\nabla\tilde{u}) + k^2\alpha\tilde{u} = 0, & \text{on} \quad \Omega_{\mathrm{PML}}^\pm := \Omega_{\mathrm{PML}} \cap \left\{x : \pm x_1 > \frac{T}{2}\right\}, \\
\tilde{u} = 0, & \text{on} \quad \Gamma^\pm := \Gamma \cap \left\{x : \pm x_1 > \frac{T}{2}\right\}, \\
\tilde{u} = 0, & \text{on} \quad \Gamma_{L+H}^\pm := \Gamma_{L+H} \cap \left\{x : \pm x_1 > \frac{T}{2}\right\}, \\
\partial_{\nu_c}\tilde{u} = g^\pm, & \text{on} \quad \Gamma_0^\pm := \Omega_{\mathrm{PML}} \cap \left\{x : x_1 = \pm\frac{T}{2}\right\},
\end{cases}
$$

for given Neumann data $g^\pm \in H^{-1/2}(\Gamma_0^\pm)$, where $\nu_c = \mathbf{A}\nu$ denotes the co-normal vector with ν pointing towards $\Omega_{\mathrm{PML}}^\pm$, $\tilde{u}$ denotes a generic field, and we note that $\Gamma^\pm \subset \Gamma_T$ does not contain the defected part Γ_0. In this section, we shall study the well-posedness of the

(a) (b)
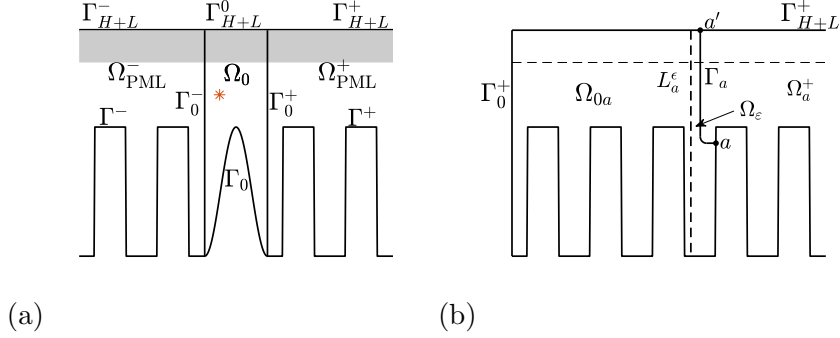
Figure 2: (a) Region Ω_{PML} is divided into three regions Ω_{PML}^-, Ω_0 and Ω_{PML}^+; semi-waveguide problems $(P^\pm)$ are defined in $\Omega^\pm$ bounded by $\Gamma_{H+L}^\pm$, $\Gamma_0^\pm$ and $\Gamma^\pm$. (b) Domain Ω_{PML}^+ is further truncated onto Ω_{0a} by a smooth curve Γ_a intersecting Γ^+ and Γ_{H+L}^+ perpendicularly at a and a', respectively. $\Omega_a^+ = \Omega_{\mathrm{PML}}^+ \backslash \overline{\Omega_{0a}}$ and the auxiliary line L_a^ϵ is chosen such that the domain Ω_ϵ is sufficiently narrow.

semi-waveguide problems $(P^\pm)$.

By Theorem 3.1, the following uniqueness result is easy to obtain.

Lemma 4.1 *Provided that $S_c L$ is sufficiently large, problem $(P^\pm)$ has at most one solution in $H^1(\Omega_{\mathrm{PML}}^\pm)$.*

Proof 3 *Suppose $\tilde{u} \in H^1(\Omega_{\mathrm{PML}}^+)$ satisfies (P^+) with $g^+ = 0$. Let*

$$
\begin{aligned}
\Omega_{\mathrm{PML}}^e &= \{x \in \mathbb{R}^2 : (x_1, x_2) \in \Omega_{\mathrm{PML}}^+ \text{ or } (T - x_1, x_2) \in \Omega_{\mathrm{PML}}^+\} \cup \Gamma_0^+, \\
\Gamma^e &= \{x \in \mathbb{R}^2 : (x_1, x_2) \in \Gamma^+ \text{ or } (T - x_1, x_2) \in \Gamma^+ \text{ or } (T/2, x_2) \in \Gamma\}.
\end{aligned}
$$

Then,

$$
\tilde{u}^e(x_1, x_2) = \begin{cases}
\tilde{u}(x_1, x_2), & x_1 \geq T/2, \\
\tilde{u}(T - x_1, x_2), & x_1 < T/2,
\end{cases}
$$

in $H^1(\Omega_{\mathrm{PML}}^e)$ satisfies problem (25-27) with $\tilde{g}$, Ω_{PML} and Γ replaced by 0, Ω_{PML}^e and Γ^e, respectively. Theorem 3.1 and Remark 3.1 imply that $\tilde{u}^e = 0$ on Ω_{PML}^e so that $\tilde{u} = \tilde{u}^e|_{\Omega_{\mathrm{PML}}^+} = 0$. The uniqueness of problem (P^-) can be established similarly.

We are ready to study the well-posedness of problem $(P^\pm)$ by the Fredholm alternative. Without loss of generality, we shall study (P^+) only. To make use of Fredholm theory, we need first to truncate Ω^+_{PML} by an exact transparent boundary condition. Under condition (GC2), there exists a line segment $L_a \subset \Gamma_T \cap \Gamma$ with the midpoint $a = (a_1, a_2) \in L_a$ for $a_1 > T/2$. For a small fixed constant $\epsilon > 0$, we can find a vertical line segment L^ϵ_a and a simple and smooth curve $\Gamma_a \subset \Omega_{\text{PML}}$ connecting L_a and Γ^+_{H+L} such that the distance of L^ϵ_a and Γ_a is ϵ and that Γ_a intersecting L_a and Γ^+_{H+L} perpendicularly at a and a', respectively, as shown in Figure 2 (b). Let Ω_ϵ be the domain bounded by Γ_a, L^ϵ_a, L_a and Γ^+_{H+L} and Ω^+_a be the unbounded domain bounded by Γ_a, Γ^+_{H+L} and Γ. For sufficiently small ϵ, the above choice of L^ϵ_a and Γ_a guarantees that $k > 0$ is not an eigenvalue of

$$-\nabla \cdot (\mathbf{A}\nabla \tilde{u}) = k^2 \alpha \tilde{u}, \quad \text{on} \quad \Omega_\epsilon, \tag{44}$$

$$\tilde{u} = 0, \quad \text{on} \quad \partial\Omega_\epsilon. \tag{45}$$

Now for the unbounded domain $\Omega^+_\epsilon = \Omega_\epsilon \cup \Gamma_a \cup \Omega^+_a$, by a symmetrical reflection w.r.t the line containing L^ϵ_a, the partial boundary $\partial\Omega^+_\epsilon \cap \Gamma$ can be extended to a Lipschitz boundary, denoted by Γ_ϵ, satisfying (GC1). Then, Theorem 3.1, with Γ_ϵ in place of Γ, can help to construct the Dirichlet Green function of Ω^+_ϵ by $\tilde{G}_{\text{D}}(x; y) = \tilde{u}^{\text{og}}(x; y) - \tilde{u}^{\text{og}}(x; y^\epsilon_{\text{imag}})$ satisfying $\tilde{G}_{\text{D}}(\cdot; y)|_{\partial\Omega^+_\epsilon} = 0$, where y^ϵ_{imag} is the mirror image of the source point y w.r.t line L^ϵ_a. Choosing Γ_a in such a special way, the following local regularity property of $\tilde{G}_{\text{D}}(x; y)$ can be ensured.

Proposition 4.1 *Under the geometrical conditions (GC1) and (GC2), for sufficiently large values of L and m in (17), $\tilde{G}_{\text{D}}(x; y)$ admits the following decomposition*

$$\tilde{G}_{\text{D}}(x; y) = \tilde{G}(x; y) - \tilde{G}(x; y^l_{\text{imag}}) + R_l(x, y), y \in \overline{\Omega_l}, \tag{46}$$

such that $R_l(x, y)$ is a sufficiently smooth function of x and y for $(x, y) \in \overline{\Omega_l \cup \Omega_c} \times \overline{\Omega_l}$, where $\tilde{G}$ is defined by (21), Ω_l is a sufficiently small neighborhood of point l in Ω^+_ϵ and y^l_{imag} is the mirror image of l w.r.t line L_l for $l = a, a'$, and Ω_c can be any bounded subset of Ω^+_ϵ.

Proof 4 *We consider y close to point a' only. Define*

$$\tilde{u}_{a'}(x; y) := \tilde{u}^{\text{og}}(x; y) - \chi_{a'}(x) \left[\tilde{G}(x; y) - \tilde{G}(x; y^{a'}_{\text{imag}}) \right],$$

where the cut-off function $\chi_{a'} = 1$ in a neighborhood of a' and has a small support that is independent of y. Then, it can be seen that $\tilde{u}_{a'}$ satisfies (25-27) with $\hat{g}^{\text{inc}}$ replaced by

$$[\nabla \cdot (\mathbf{A}\nabla) + k^2 \alpha](1 - \chi_{a'}(x)) \left[\tilde{G}(x; y) - \tilde{G}(x; y^{a'}_{\text{imag}}) \right] \in C^{m-1}_{\text{comp}}(\Omega_{\text{PML}} \times \overline{\Omega_l}),$$

where C^{m-1}_{comp} consists of $m-1$ times differentiable functions with compact supports, and we note that m defined in (17) determines the smoothness of σ. By arguing the same way as in [18, Lem 2.4] and by choosing m sufficiently large, $R_{a'}(x, y) = \tilde{u}_{a'}(x; y) - \tilde{u}^{\text{og}}(x; y^\epsilon_{\text{imag}})$ becomes a sufficiently smooth function for $(x, y) \in \overline{\Omega_l \cup \Omega_c} \times \overline{\Omega_l}$.

On Γ_a, we now define the following two integral operators:

$$[\mathcal{S}_a\phi](x) = 2\int_{\Gamma_a} \tilde{G}_{\text{D}}(x; y)\phi(y)ds(y), \tag{47}$$

$$[\mathcal{K}_a\phi](x) = 2\int_{\Gamma_a} \partial_{\nu_c(y)}\tilde{G}_{\text{D}}(x; y)\phi(y)ds(y), \tag{48}$$

Proposition 4.1 reveals that classic mapping properties hold for the above two integral operators on the open arc Γ_a.

12

Lemma 4.2 *We can uniquely extend the operator $\mathcal{S}_a$ as a bounded operator from $H^{-1/2}(\Gamma_a)$ to $\widetilde{H^{1/2}}(\Gamma_a)$, the operator $\mathcal{K}_a$ as a compact (and certainly bounded) operator from $\widetilde{H^{1/2}}(\Gamma_a)$ to $\widetilde{H^{1/2}}(\Gamma_a)$. Moreover, we have the decomposition $\mathcal{S}_a = \mathcal{S}_{p,a} + \mathcal{L}_{p,a}$ such that $\mathcal{S}_{p,a} : H^{-1/2}(\Gamma_a) \to \widetilde{H^{1/2}}(\Gamma_a)$ is positive and bounded below, i.e., for some constant $c > 0$,*

$$\mathrm{Re}\left(\int_{\Gamma_a} \mathcal{S}_{p,a}\phi\bar{\phi}ds\right) \geq c||\phi||^2_{H^{-1/2}(\Gamma_a)},$$

for any $\phi \in H^{-1/2}(\Gamma_a)$, and $\mathcal{L}_{p,a} : H^{-1/2}(\Gamma_a) \to \widetilde{H^{1/2}}(\Gamma_a)$ is compact.

Proof 5 *By Proposition 4.1, the proof follows from similar arguments as in [18, Sec. 2.3] but relies on Fredholm of the single-layer potential and compactness of the double-layer potential of kernels relating to $\tilde{G}$, the fundamental solution of the strongly elliptic Helmholtz equation (18), as has been studied in [30, Thm. 7.6] and [23]. We omit the details.*

Analogous to [23, Lem. 5.1], one gets the following the Green's representation

$$\tilde{u}(x) = \int_{\Gamma_a} \left[\partial_{\nu_c(y)}\tilde{G}_{\mathrm{D}}(x; y)\tilde{u}(y) - \tilde{G}_{\mathrm{D}}(x; y)\partial_{\nu_c(y)}\tilde{u}(y)\right] ds(y). \tag{49}$$

By the jump relations [23, Thm. 5.1], letting x approach Γ_a, we get the following transparent boundary condition (TBC)

$$\tilde{u} - \mathcal{K}_a\tilde{u} = -\mathcal{S}_a\partial_{\nu_c}\tilde{u}, \quad \text{on} \quad \Gamma_a. \tag{50}$$

As indicated in Figure 2 (b), let Ω_{0a} be the domain bounded by Γ_0^+, Γ_a, Γ_{H+L}^+ and Γ_+,

$$H_D^1(\Omega_{0a}) = \{v|_{H^1(\Omega_{0a})} : v \in H^1(\Omega_{\mathrm{PML}}^+), v|_{\Gamma_+} = 0, v|_{\Gamma_{H+L}} = 0\},$$

and $V_a = H_D^1(\Omega_{0a}) \times H^{-1/2}(\Gamma_a)$ be equipped with the natural cross-product norm. (P^+) can be equivalently formulated as the following boundary value problem: find $(\tilde{u}, \phi) \in V_a$ solving

$$\nabla \cdot (\mathbf{A}\nabla\tilde{u}) + k^2\alpha\tilde{u} = 0, \quad \text{on} \quad \Omega_{0a}, \tag{51}$$

$$\partial_{\nu_c}\tilde{u}|_{\Gamma_0^+} = g^+, \quad \text{on} \quad \Gamma_0^+, \tag{52}$$

$$\partial_{\nu_c}\tilde{u}|_{\Gamma_a} = \phi, \quad \text{on} \quad \Gamma_a, \tag{53}$$

$$\tilde{u} - \mathcal{K}_a\tilde{u} = -\mathcal{S}_a\phi, \quad \text{on} \quad \Gamma_a. \tag{54}$$

An equivalent variational formulation reads: find $(\tilde{u}, \phi) \in V_a$ such that

$$b_{ps}((\tilde{u}, \phi), (v, \psi)) = \int_{\Gamma_0^+} g^+\bar{v}ds, \tag{55}$$

for all $(v, \psi) \in V_a$, where the sesquilinear form $b_{ps}(\cdot, \cdot) : V_a \times V_a \to \mathbb{C}$ is given by

$$b_{ps}((\tilde{u}, \phi), (v, \psi)) = \int_{\Omega_{0a}} \left[(\mathbf{A}\nabla\tilde{u})^T\overline{\nabla v} - k^2\alpha\tilde{u}\bar{v}\right] dx - \int_{\Gamma_a} \left[\phi\bar{v} - (\tilde{u} - \mathcal{K}_a\tilde{u} + \mathcal{S}_a\phi)\bar{\psi}\right] ds.$$

We are now ready to establish the well-posedness of problems (P^+).

Theorem 4.1 *Under the geometrical conditions (GC1) and (GC2), provided that L is sufficiently large, the semi-waveguide problem $(P^\pm)$ has a unique solution $\tilde{u} \in H^1(\Omega_{\mathrm{PML}}^\pm)$ such that $||\tilde{u}||_{H^1(\Omega_{\mathrm{PML}}^\pm)} \le C||g^\pm||_{H^{-1/2}(\Gamma_0^\pm)}$ for any $g^\pm \in H^{-1/2}(\Gamma_0^\pm)$, respectively, where C is independent of $g^\pm$.*

Proof 6 *We study (P^+) only. For the variational problem (55), we can decompose $b_{ps} = b_1 + b_2$ where*

$$b_1((\tilde{u},\phi),(v,\psi)) = \int_{\Omega_{0a}} \left[(\mathbf{A}\nabla\tilde{u})^T\overline{\nabla v} - k^2\alpha\tilde{u}\bar{v}\right]dx - \int_{\Gamma_a}\left[\phi\bar{v} - \tilde{u}\bar{\psi} - \mathcal{S}_{p,a}\phi\bar{\psi}\right]ds,$$

$$b_2((\tilde{u},\phi),(v,\psi)) = \int_{\Gamma_a}[\mathcal{L}_{p,a}\phi - \mathcal{K}_a\phi]\,\bar{\psi}ds.$$

According to Lemma 4.2, b_1 is coercive on V as

$$\mathrm{Re}(b_1((\tilde{u},\phi),(\tilde{u},\phi))) = \int_{\Omega_{0a}}\left[|\tilde{u}_{x_1}|^2 + (1+\sigma^2(x_2))^{-1}|\tilde{u}_{x_2}|^2 - k^2|\tilde{u}|^2\right]dx + \mathrm{Re}\left(\int_{\Gamma_a}\mathcal{S}_{p,a}\phi\bar{\phi}ds\right)$$
$$\ge c||\tilde{u}||_{H^1(\Omega_{0a})}^2 - C||\tilde{u}||_{L^2(\Omega_{0a})}^2 + c||\phi||_{H^{-1/2}(\Gamma_a)}^2,$$

and the bounded linear operator associated with b_2 is compact. Consequently, b_{ps} is Fredholm of index zero [30, Thm. 2.34].

Now, we prove $\tilde{u} = 0$ and $\phi = 0$ when $g^+ = 0$. By (49), we can directly extend $\tilde{u}$ to Ω_ϵ^+, denoted by $\tilde{u}^{\mathrm{ext}}$. Then, the TBC (50) implies $\gamma^+\tilde{u}^{\mathrm{ext}}|_{\Omega_a^+} = \tilde{u}|_{\Gamma_a}$ so that by the jump relations, $\gamma^-\tilde{u}^{\mathrm{ext}}|_{\Omega_\epsilon} = 0$ where γ^+ (γ^-) defines the trace operator of $\tilde{u}^{\mathrm{ext}}$ onto Γ_a from Ω_a^+ (Ω_ϵ). Thus, $\tilde{u}^- = \tilde{u}^{\mathrm{ext}}|_{\Omega_\epsilon}$ satisfies (44) and (45). But the special choice of ϵ and Ω_ϵ has ensured that $\tilde{u}^- \equiv 0$ on Ω_ϵ so that the trace of $\partial_{\nu_c}\tilde{u}^{\mathrm{ext}}$ taken from Ω_ϵ is 0. The jump conditions then imply that the trace of $\partial_{\nu_c}\tilde{u}^{\mathrm{ext}}$ taken from Ω_a^+ is ϕ. Consequently,

$$w(x) = \begin{cases} \tilde{u}(x), & x \in \Omega_{0a}, \\ \tilde{u}^{\mathrm{ext}}(x), & x \in \Omega_a^+, \end{cases}$$

belongs to $H^1(\Omega_{\mathrm{PML}}^+)$ and satisfies (P^+) with $g^+ = 0$. But Lemma 4.1 already justifies that w must be 0 on Ω_{PML}^+, which indicates that $\tilde{u} = 0$ and $\phi = 0$. The proof then follows from the fact that the right-hand side of (55) defines a bounded anti-linear functional in V_a^*.

Remark 4.1 *Like Therorem 3.1, Theorem 4.1 also holds for any Lipschitz curves $\Gamma^\pm$, which are not necessarily periodic, satisfying the geometrical conditions (GC1) and (GC2).*

5 Lateral boundary conditions

According to Theorem 3.1, $\partial_{\nu_c}\tilde{u}^{\mathrm{og}}(\cdot;x^*)|_{\Gamma_0}^\pm \in H^{-1/2}(\Gamma_0^\pm)$ for any $x^* \in S_H$ with $|x_1^*| < T/2$. Thus, $\tilde{u} = \tilde{u}^{\mathrm{og}}(\cdot;x^*)|_{\Omega_{\mathrm{PML}}^\pm}$ satisfies $(P^\pm)$ with $g^\pm = \partial_{\nu_c}\tilde{u}^{\mathrm{og}}(\cdot;x^*)|_{\Gamma_0}^\pm$ in the distributional sense, respectively. Theorem 4.1 then implies that we can define two vertical Neumann-to-Dirichlet (vNtD) operators $\mathcal{N}^\pm : H^{-1/2}(\Gamma_0^\pm) \to \widetilde{H^{1/2}}(\Gamma_0^\pm)$ satisfying $\tilde{u}^{\mathrm{og}}|_{\Gamma_0^\pm} = \mathcal{N}^\pm\partial_{\nu_c}\tilde{u}^{\mathrm{og}}|_{\Gamma_0^\pm}$. Such transparent boundary conditions can serve as exact *lateral boundary conditions* to terminate the x_1-variable for the PML-truncated problem (18) and (19). Consequently, the original unbounded problem (1) and (2) equipped with the

hSRC condition (9) can be truncated onto the perturbed cell $\Omega_0 := \Omega_{\text{PML}} \cap \{x : |x_1| < \frac{T}{2}\}$ and be reformulated as the following boundary value problem:

$$\text{(BVP1)} : \begin{cases} \nabla \cdot (\mathbf{A}\nabla \tilde{u}^{\text{og}}) + k^2 \alpha \tilde{u}^{\text{og}} = -\delta(x - x^*), & \text{on } \Omega_0, \\ \tilde{u}^{\text{og}} = 0, & \text{on } \Gamma_0 = \Gamma \cap \{x : |x_1| < T/2\}, \\ \tilde{u}^{\text{og}} = 0, & \text{on } \Gamma_{H+L}^0 = \Gamma_{H+L} \cap \{x : |x_1| < T/2\}, \\ \tilde{u}^{\text{og}} = \mathcal{N}^{\pm} \partial_{\nu_c} \tilde{u}^{\text{og}}, & \text{on } \Gamma_0^{\pm}. \end{cases}$$

Theorems 3.1 and 4.1 directly imply that (BVP1) admits the following unique solution

$$\tilde{u}^{\text{og}}(\cdot ; x^*) = \tilde{u}_r^{\text{og}}(\cdot ; x^*)|_{\Omega_0} + \chi(\cdot ; x^*)|_{\Omega_0} \tilde{u}^{\text{inc}}(x ; x^*)|_{\Omega_0},$$

with $\tilde{u}_r^{\text{og}}$ defined in Theorem 3.1. Nevertheless, it is challenging to get $\mathcal{N}^{\pm}$ by directly solving the unbounded problem $(P^{\pm})$ in practice. To overcome this difficulty, in this section, we shall define two closely related Neumann-marching operators, derive the governing Riccati equations, and design an efficient RDP to accurately approximate $\mathcal{N}^{\pm}$.

5.1 Neumann-marching operators $\mathcal{R}_p^{\pm}$

Now, let

$$\Gamma_j^{\pm} = \{(x_1 \pm jT, x_2) :, x = (x_1, x_2) \in \Gamma_0^{\pm}\},$$
$$\Omega_{\text{PML},j}^{\pm} = \{x \in \Omega_{\text{PML}}^{\pm} : \pm x_1 > T/2 + (j - 1)T\},$$
$$\Omega_j^{\pm} = \Omega_{\text{PML},j}^{\pm} \backslash \overline{\Omega_{\text{PML},j+1}^{\pm}}$$

for $j \in \mathbb{N}^*$, as illustrated in Figure 3(a) for the notations of superscript $+$.

(a) (b)
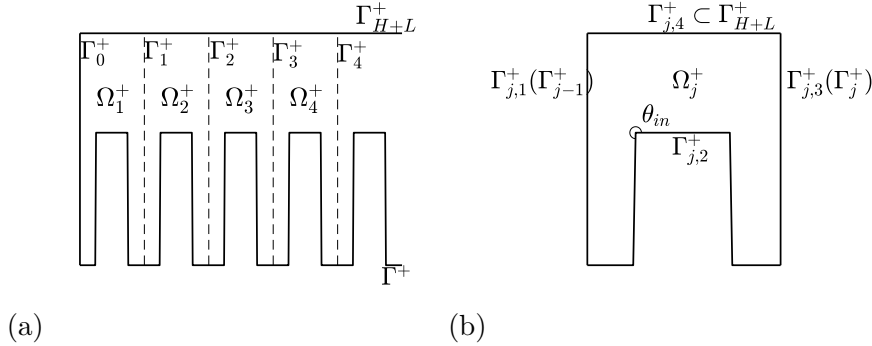
Figure 3: (a) The semi-waveguide region Ω_{PML}^+ is divided into $\{\Omega_j^+\}_{j=1}^{\infty}$ of the same shape. The operator $\mathcal{R}_p^+$ can then march Neumann data through the vertical line segments $\{\Gamma_j^+\}_{j=0}^{\infty}$. (b) The boundary of Ω_j consists of four parts: $\Gamma_{j,1}^+$ (left), $\Gamma_{j,2}^+$ (bottom), $\Gamma_{j,3}^+$ (right), $\Gamma_{j,4}^+$ (top). Here, θ^{in} indicates the interior angle at a corner, as will be used in (86).

As insipired by [21], the well-posedness of $(P^{\pm})$ well defines two bounded Neumann-marching operators $\mathcal{R}_p^{\pm} : H^{-1/2}(\Gamma_0^{\pm}) \to H^{-1/2}(\Gamma_1^{\pm})$ such that $\partial_{\nu_c^{\pm}} \tilde{u}^{\text{og}}|_{\Gamma_1^{\pm}} = \mathcal{R}_p^{\pm} \partial_{\nu_c^{\pm}} \tilde{u}^{\text{og}}|_{\Gamma_0^{\pm}}$, where $\nu_c^{\pm} = \mathbf{A}\nu^{\pm}$ with $\nu^{\pm} = (\pm 1, 0)^T$. We have the following properties of $\mathcal{R}_p^{\pm}$, analogous to [21, Thm. 3.1].

Proposition 5.1 *Under the conditions that (GC2) holds and kL is sufficiently large, we can choose $\Gamma_0^{\pm}$ intersecting Γ at a smooth point such that $\mathcal{R}_p^{\pm}$ are compact operators and*

$$\partial_{\nu_c^{\pm}} \tilde{u}^{\text{og}}|_{\Gamma_{j+1}^{\pm}} = \mathcal{R}_p^{\pm} \partial_{\nu_c^{\pm}} \tilde{u}^{\text{og}}|_{\Gamma_j^{\pm}}, \tag{56}$$

15

holds for any $j \geq 0$. Furthermore,

$$\rho(\mathcal{R}_p^{\pm}) < 1, \qquad (57)$$

where ρ denotes the spectral radius.

Proof 7 *We study only the property of $\mathcal{R}_p^+$. The choice of Γ_0^+ and the interior regularity theory of elliptic operators directly imply the compactness of $\mathcal{R}_p^+$.*

It is clear that (56) holds for $j = 0$. We need only justify the case $j = 1$ as all others can be done by induction. Consider the semi-waveguide problem (P^+) with $g^+ = -\partial_{\nu_c^+} \tilde{u}^{\mathrm{og}}|_{\Gamma_1^+}$, where the negative sign appears since $\nu_c^+ = -\nu_c$. Theorem 4.1 implies that $\tilde{u}_n^{\mathrm{og}}(x) = \tilde{u}^{\mathrm{og}}(x_1 + T, x_2)$ for $x \in \Omega_{\mathrm{PML}}^+$ is the unique solution. Then $\partial_{\nu_c^+} \tilde{u}_n^{\mathrm{og}}|_{\Gamma_1^+} = \mathcal{R}_p^+ \partial_{\nu_c^+} \tilde{u}_n^{\mathrm{og}}|_{\Gamma_0^+}$, which reads exactly $\partial_{\nu_c^+} \tilde{u}^{\mathrm{og}}|_{\Gamma_2^+} = \mathcal{R}_p^+ \partial_{\nu_c^+} \tilde{u}^{\mathrm{og}}|_{\Gamma_1^+}$.

Now we prove (57) by contradiction. Suppose otherwise there exists $0 \neq g \in H^{-1/2}(\Gamma_0^+)$ such that $\mathcal{R}_p^+ g = \lambda_0 g$ with $|\lambda_0| \geq 1$. Suppose $\tilde{u}$ satisfies (P^+) with $g^+ = g$ on Γ_0^+. Then, for any $v \in H^1(\Omega_{\mathrm{PML}}^+)$ so that $v(\cdot - jT, \cdot) \in H^1(\Omega_{\mathrm{PML},j+1}^+)$ for any $j \geq 0$, we have by Green's identity that,

$$|\lambda_0|^j \left| \int_{\Gamma_0} g\bar{v} ds \right| = \left| \int_{\Gamma_j} (\mathcal{R}_p^+)^j g \overline{v(\cdot - jT, \cdot)} ds \right|$$

$$= \left| \int_{\Omega_{\mathrm{PML},j+1}} \left[(\mathbf{A}\nabla\tilde{u}^{\mathrm{og}})^T \overline{\nabla v(\cdot - jT, \cdot)} - k^2 \alpha \tilde{u}^{\mathrm{og}} \overline{v(\cdot - jT, \cdot))} \right] dx \right|$$

$$\leq C \|\tilde{u}^{\mathrm{og}}\|_{H^1(\Omega_{\mathrm{PML},j+1}^+)} \|v\|_{H^1(\Omega_{\mathrm{PML}}^+)} \to 0, \quad j \to \infty,$$

which is impossible.

By the following identity [22],

$$\rho(\mathcal{R}_p^{\pm}) = \lim_{j \to \infty} \|(\mathcal{R}_p^{\pm})^j\|^{1/j},$$

it can be seen that there exists a sufficiently large integer $N_0 > 0$ such that $(\mathcal{R}_p^{\pm})^{N_0}$ is contracting, i.e.,

$$\|(\mathcal{R}_p^{\pm})^{N_0}\| < 1. \qquad (58)$$

Let $\Omega_j^{\pm,N_0}$ be the interior of N_0 consecutive cells $\cup_{j'=1}^{N_0} \overline{\Omega_{(j-1)N_0+j'}^{\pm}}$. As a corollary, the above results indicate that $\tilde{u}^{\mathrm{og}}$ decays exponentially at infinity of the strip.

Corollary 5.1 *Under the conditions that (GC2) holds and kL is sufficiently large,*

$$\|\tilde{u}^{\mathrm{og}}(\cdot; x^*)\|_{H^1(\Omega_j^{\pm,N_0})} \leq C \|(\mathcal{R}_p^{\pm})^{N_0}\|^{j-1} \|\tilde{g}^{\mathrm{inc}}\|_{L^2(\Omega_{\mathrm{PML}})}, \qquad (59)$$

where we recall that $\tilde{g}^{\mathrm{inc}} = [\nabla \cdot (\mathbf{A}\nabla) + k^2\alpha](1 - \chi(x; x^*))\tilde{u}^{\mathrm{inc}}(x; x^*)$, and C is independent of $j \geq 0$. In other words, the PML truncated solution $\tilde{u}^{\mathrm{og}}(x; x^*)$ decays exponentially fast to 0 in the strip as $|x_1| \to \infty$ for any $x^* \in \Omega_{\mathrm{PML}}$.

Remark 5.1 *Authors in [6] have revealed a similar result as (59) for Γ being a flat surface. The above corollary indicates that such an exponentially decaying property for the PML truncated solution holds even for locally defected periodic curves. As a consequence, this reveals that the PML truncation cannot realize an exponential convergence to the true solution for numerical solutions at regions sufficiently away from the source or local defects since the true solution is expected to decay only of an algebraic rate at infinity: [7] has indicated that u^{og} behaves as $\mathcal{O}(x_1^{-3/2})$ as $x_1 \to \infty$.*

Though Corollary 5.1 provides hopeless results, we point out that (59) holds for L being fixed but $j \to \infty$. If, on the contrary, j is fixed but $L \to \infty$, we believe exponential convergence can still be achieved. In doing so, we need a more effective description of the Neumann-marching operators $\mathcal{R}_p^\pm$, as was done in [21]. Take $\mathcal{R}_p^+$ as an example. As shown in Figure 3(b), recall that Ω_j^+ denotes the j-th unit cell on the right of Γ_0^+, which is unperturbed for $j \geq 1$, and to simplify the presentation, we further denote the four boundaries of Ω_j^+ by

$$\Gamma_{j,1} = \Gamma_{j-1}^+, \quad \Gamma_{j,3} = \Gamma_j^+, \quad \Gamma_{j,2} = \overline{\Omega_j^+} \cap \Gamma, \quad \Gamma_{j,4} = \overline{\Omega_j^+} \cap \Gamma_{H+L}^+.$$

Consider the following boundary value problem for a generic field $\tilde{u}$:

$$\text{(BVP2)}: \quad \begin{cases} \nabla \cdot (\mathbf{A} \nabla \tilde{u}) + k^2 \alpha \tilde{u} = 0, & \text{on } \Omega_j^+, \\ \tilde{u} = 0, & \text{on } \Gamma_{j,2} \cup \Gamma_{j,4}, \\ \partial_{\nu_c} \tilde{u} = g_i, & \text{on } \Gamma_i^+, i = j-1, j, \end{cases}$$

for $g_i \in H^{-1/2}(\Gamma_i^+), i = j-1, j$. We have the following well-posedness theorem.

Theorem 5.1 *Provided that $kT/\pi \notin \mathcal{E} := \{i'/2^{j'} | j' \in \mathbb{N}, i' \in \mathbb{N}^*\}$, and L is sufficiently large, (BVP2) is well-posed. The well-posedness even holds with Ω_j^+ replaced by the interior domain of 2^l consecutive cells, say $\cup_{j=1}^{2^l} \overline{\Omega_j^+}$, for any number $l \geq 0$.*

Proof 8 *It is clear that only uniqueness is needed [30, Thm. 4.10]. Suppose $j = 1$ and $g_i = 0, i = 0, 1$. Then, by first an even extension over Γ_0^+ and then a $2T$-periodic extension, we get a $2T$-periodic solution $\tilde{u}^e$ (corresponding to a normal incidence) in a strip bounded in the x_2-direction by a $2T$-periodic grating surface, possibly different from Γ, and Γ_{H+L}. However, according to the well-posedness theory [5, Cor. 5.2] for the half-space scattering by the grating, the PML convergence theory in [10, Thm. 2.4] can be readily adapted here to show that $\tilde{u}^e \equiv 0$, considering that $kT/\pi \notin \mathcal{E}$ has excluded horizontally propagating Bloch modes.*

Remark 5.2 *We note that the condition $kT/\pi \notin \mathcal{E}$ is not necessary for the well-posedness of (BVP2). Even if $kT/\pi \in \mathcal{E}$, one may impose zero Neumann condition on $\Gamma_{4,j}$ to guarantee the uniqueness of the modified (BVP2) [29, 34].*

By Theorem 5.1, we can define a bounded Neumann-to-Dirichlet operator $\mathcal{N}^{(0)} : H^{-1/2}(\Gamma_{j-1}^+) \times H^{-1/2}(\Gamma_j^+) \to \widetilde{H^{1/2}}(\Gamma_{j-1}^+) \times \widetilde{H^{1/2}}(\Gamma_j^+)$ such that

$$\begin{bmatrix} \tilde{u}|_{\Gamma_{j-1}^+} \\ \tilde{u}|_{\Gamma_j^+} \end{bmatrix} = \mathcal{N}^{(0)} \begin{bmatrix} \partial_{\nu_c^-} \tilde{u}|_{\Gamma_{j-1}^+} \\ \partial_{\nu_c^+} \tilde{u}|_{\Gamma_j^+} \end{bmatrix}, \tag{60}$$

for all $j \geq 1$. Due to the invariant shape of Ω_j^+ with respect to j, $\mathcal{N}^{(0)}$ is in fact independent of j. Suppose $j = 1$. Then, by the linearity principle, $\mathcal{N}^{(0)}$ can be rewritten in the following matrix form

$$\mathcal{N}^{(0)} = \begin{bmatrix} \mathcal{N}_{00}^{(0)} & \mathcal{N}_{01}^{(0)} \\ \mathcal{N}_{10}^{(0)} & \mathcal{N}_{11}^{(0)} \end{bmatrix},$$

where the bounded map $\mathcal{N}_{i'j'}^{(0)} : H^{-1/2}(\Gamma_{j'}^+) \to \widetilde{H^{1/2}}(\Gamma_{i'})$ maps $\partial_{\nu_c} \tilde{u}|_{\Gamma_{j'}^+} = g_{j'}$ to $\tilde{u}|_{\Gamma_{i'}^+}$ if $g_{1-j'} = 0$ for $i', j' = 0, 1$.

Due to the shape invariance of Γ_j^+, we shall identify $H^{-1/2}(\Gamma_j^+)$ for all $j \geq 0$ as the same space $H^{-1/2}(\Gamma_0^+)$, and, similarly, the $\widetilde{H^{1/2}}(\Gamma_j^+)$ shall all be identified as the dual space of $H^{-1/2}(\Gamma_0^+)$.

Returning back to the semi-waveguide problems $(P^\pm)$, we have, by the definition of $\mathcal{R}_p^+$ and (60) for $j = 1$ and 2, that

$$\mathcal{N}_{10}^{(0)}\partial_{\nu_c^-}\tilde{u}^{\mathrm{og}}|_{\Gamma_0^+} - \mathcal{N}_{11}^{(0)}\mathcal{R}_p^+\partial_{\nu_c^-}\tilde{u}^{\mathrm{og}}|_{\Gamma_0^+} = \tilde{u}^{\mathrm{og}}|_{\Gamma_1^+} = \mathcal{N}_{00}^{(0)}\mathcal{R}_p^+\partial_{\nu_c^-}\tilde{u}^{\mathrm{og}}|_{\Gamma_0^+} - \mathcal{N}_{01}^{(0)}(\mathcal{R}_p^+)^2\partial_{\nu_c^-}\tilde{u}^{\mathrm{og}}|_{\Gamma_0^+}. \tag{61}$$

Here and in the following, the product of two operators should be regarded as their composition. Thus,

$$\left[\mathcal{N}_{10}^{(0)} + \mathcal{N}_{11}^{(0)}\mathcal{R}_p^+ + \mathcal{N}_{00}^{(0)}\mathcal{R}_p^+ + \mathcal{N}_{01}^{(0)}(\mathcal{R}_p^+)^2\right]\partial_{\nu_c}\tilde{u}^{\mathrm{og}}|_{\Gamma_0^+} = 0,$$

for any $\partial_{\nu_c}\tilde{u}^{\mathrm{og}}|_{\Gamma_0^+} \in H^{-1/2}(\Gamma_0^+)$, so that we end up with the following Riccati equation for $\mathcal{R}_p^+$:

$$\mathcal{N}_{10}^{(0)} + [\mathcal{N}_{11}^{(0)} + \mathcal{N}_{00}^{(0)}]\mathcal{R}_p^+ + \mathcal{N}_{01}^{(0)}(\mathcal{R}_p^+)^2 = 0. \tag{62}$$

One similarly obtains the governing equation for $\mathcal{R}_p^-$:

$$\mathcal{N}_{01}^{(0)} + [\mathcal{N}_{11}^{(0)} + \mathcal{N}_{00}^{(0)}]\mathcal{R}_p^- + \mathcal{N}_{10}^{(0)}(\mathcal{R}_p^-)^2 = 0. \tag{63}$$

Analogous to [21], the previous results in fact indicate that the two Riccati equations (62) and (63) must be uniquely solvable under the condition that $\rho(R_p^\pm) < 1$. The vNtD operators $\mathcal{N}^\pm$ mapping $\partial_{\nu_c}\tilde{u}^{\mathrm{og}}|_{\Gamma_0^\pm}$ to $\tilde{u}^{\mathrm{og}}|_{\Gamma_0^\pm}$ are respectively given by

$$\mathcal{N}^+ = \mathcal{N}_{00}^{(0)} - \mathcal{N}_{01}^{(0)}\mathcal{R}_p^+, \tag{64}$$

$$\mathcal{N}^- = \mathcal{N}_{11}^{(0)} - \mathcal{N}_{10}^{(0)}\mathcal{R}_p^-. \tag{65}$$

However, due to the nonlinearity of the Riccati equations (62) and (63), it is not that easy to get $\mathcal{N}^\pm$ in practice [21]. To tackle this difficulty, we shall develop an RDP to effectively approximate $\mathcal{R}_p^\pm$.

5.2 Recursive doubling procedure

Take $\mathcal{R}_p^+$ as an example. We first study the NtD operator

$$\mathcal{N}^{(l)} = \begin{bmatrix} \mathcal{N}_{00}^{(l)} & \mathcal{N}_{01}^{(l)} \\ \mathcal{N}_{10}^{(l)} & \mathcal{N}_{11}^{(l)} \end{bmatrix} \tag{66}$$

on the boundary of $\cup_{j=1}^{2^l}\overline{\Omega_j^+}$ for $l \geq 1$, where $\mathcal{N}_{i'j'}^{(l)}$ is bounded from $H^{-1/2}(\Gamma_0^+)$ to $\widetilde{H^{1/2}}(\Gamma_0)$ for $i', j' = 0, 1$. If $l = 1$, we need to compute $\mathcal{N}^{(1)}$ on the boundary of $\overline{\Omega_1^+ \cup \Omega_2^+}$. Using (60) for $j = 1$ and 2 and eliminating $\tilde{u}^{\mathrm{og}}$ and $\partial_{\nu_c}\tilde{u}^{\mathrm{og}}$ by the continuity condition on Γ_1^+, one gets

$$(\mathcal{N}_{00}^{(l-1)} + \mathcal{N}_{11}^{(l-1)})\partial_{\nu_c^+}\tilde{u}^{\mathrm{og}}|_{\Gamma_1^+} = -\mathcal{N}_{10}^{(l-1)}\partial_{\nu_c^-}\tilde{u}^{\mathrm{og}}|_{\Gamma_0^+} + \mathcal{N}_{01}^{(l-1)}\partial_{\nu_c^+}\tilde{u}^{\mathrm{og}}|_{\Gamma_2^+}. \tag{67}$$

By Theorem 5.1 , the well-posedness of the modified (BVP2) for $l = 1$, indicates that there exist two bounded operators $\mathcal{A}_{l-1}, \mathcal{B}_{l-1} : H^{-1/2}(\Gamma_0^+) \to H^{-1/2}(\Gamma_0^+)$ such that

$$\partial_{\nu_c^+}\tilde{u}^{\mathrm{og}}|_{\Gamma_1^+} = -\mathcal{A}_{l-1}\partial_{\nu_c^-}\tilde{u}^{\mathrm{og}}|_{\Gamma_0^+} + \mathcal{B}_{l-1}\partial_{\nu_c^+}\tilde{u}^{\mathrm{og}}|_{\Gamma_2^+}.$$

Equation (67) implies that

$$\mathcal{A}_{l-1} = (\mathcal{N}_{00}^{(l-1)} + \mathcal{N}_{11}^{(l-1)})^{-1}\mathcal{N}_{10}^{(l-1)}, \quad \mathcal{B}_{l-1} = (\mathcal{N}_{00}^{(l-1)} + \mathcal{N}_{11}^{(l-1)})^{-1}\mathcal{N}_{01}^{(l-1)},$$

where $(\mathcal{N}_{00}^{(l-1)} + \mathcal{N}_{11}^{(l-1)})^{-1}$ is a generalized inverse from $\widetilde{H^{1/2}}(\Gamma_0)$ to $H^{-1/2}(\Gamma_0^+)$. Thus, one obtains

$$\mathcal{N}_{00}^{(l)} = \mathcal{N}_{00}^{(l-1)} - \mathcal{N}_{01}^{(l-1)}\mathcal{A}_{l-1}, \quad \mathcal{N}_{01}^{(l)} = \mathcal{N}_{01}^{(l-1)}\mathcal{B}_{l-1}, \tag{68}$$

$$\mathcal{N}_{10}^{(l)} = \mathcal{N}_{10}^{(l-1)}\mathcal{A}_{l-1}, \quad \mathcal{N}_{11}^{(l)} = \mathcal{N}_{11}^{(l-1)} - \mathcal{N}_{10}^{(l-1)}\mathcal{B}_{l-1}. \tag{69}$$

Equations (68-69) can be recursively applied to get $\mathcal{N}^{(l)}$ for all $l \geq 1$, and the number of consecutive cells $\{\Omega_j\}$ doubles after each iteration, which form the origin of the term "*recursive doubling procedure*" (RPD) in the literature [33, 15]. In the following, we shall see that RDP provides a simple approach for solving (62) and (63).

Now, analogous to (62), we obtain from $\mathcal{N}^{(l)}$ and (56) the following equations

$$\mathcal{N}_{10}^{(l)} + [\mathcal{N}_{11}^{(l)} + \mathcal{N}_{00}^{(l)}](\mathcal{R}_p^+)^{2^l} + \mathcal{N}_{01}^{(l)}(\mathcal{R}_p^+)^{2^{(l+1)}} = 0, \tag{70}$$

$$\mathcal{N}^+ = \mathcal{N}_{00}^{(l)} - \mathcal{N}_{01}^{(l)}(\mathcal{R}_p^+)^{2^l}. \tag{71}$$

Since $||(\mathcal{R}_p^+)^{N_0}|| < 1$, the third term in (70) is expected to be exponentially small for $l \gg \log_2 N_0$, so that we approximate

$$(\mathcal{R}_p^+)^{2^l} \approx -[\mathcal{N}_{11}^{(l)} + \mathcal{N}_{00}^{(l)}]^{-1}\mathcal{N}_{10}^{(l)}, \tag{72}$$

$$\mathcal{N}^+ \approx \mathcal{N}_{00}^{(l)} + \mathcal{N}_{01}^{(l)}[\mathcal{N}_{11}^{(l)} + \mathcal{N}_{00}^{(l)}]^{-1}\mathcal{N}_{10}^{(l)}, \tag{73}$$

and we get $\mathcal{R}_p^+$ iteratively from

$$(\mathcal{R}_p^+)^{2^j} = -[\mathcal{N}_{11}^{(j)} + \mathcal{N}_{00}^{(j)}]^{-1}\left[\mathcal{N}_{10}^{(j)} - \mathcal{N}_{01}^{(j)}(\mathcal{R}_p^+)^{2^{j+1}}\right], \quad j = l-1, \cdots, 0. \tag{74}$$

One similarly obtains $\mathcal{N}^-$ and $\mathcal{R}_p^-$ from

$$(\mathcal{R}_p^-)^{2^l} \approx -[\mathcal{N}_{11}^{(l)} + \mathcal{N}_{00}^{(l)}]^{-1}\mathcal{N}_{01}^{(l)}, \tag{75}$$

$$\mathcal{N}^- \approx \mathcal{N}_{11}^{(l)} + \mathcal{N}_{01}^{(l)}[\mathcal{N}_{11}^{(l)} + \mathcal{N}_{00}^{(l)}]^{-1}\mathcal{N}_{10}^{(l)}, \tag{76}$$

$$(\mathcal{R}_p^-)^{2^j} = -[\mathcal{N}_{11}^{(j)} + \mathcal{N}_{00}^{(j)}]^{-1}\left[\mathcal{N}_{01}^{(j)} - \mathcal{N}_{10}^{(j)}(\mathcal{R}_p^-)^{2^{j+1}}\right], \quad j = l-1, \cdots, 0. \tag{77}$$

From the above, it can be seen that the essential step to approximate $\mathcal{N}^\pm$ is to get the NtD operator $\mathcal{N}^{(0)}$ on the boundary of any unperturbed unit cell $\Omega_j^\pm$ for $j \in \mathbb{Z}^+$. As no information of the field $\tilde{u}^{\mathrm{og}}$ in $\Omega_j^\pm$ is required, it is clear that the BIE method is an optimal choice, as it treats only the boundary of $\Omega_j^\pm$. Since PML is involved in domain $\Omega_j^\pm$, the high-accuracy PML-based BIE method developed in our previous work [28] straightforwardly provides an accurate approximation of $\mathcal{N}^{(0)}$, so as to effectively drive RDP to get $\mathcal{N}^\pm$. We shall present the details in the next section.

6   The PML-based BIE method

In this section, we shall first review the PML-based BIE method in [28] to approximate the NtD operator on the boundary of any unit cell, perturbed or not, by an NtD matrix.

Then, we shall use these NtD matrices to approximate the two vNtD operators $\mathcal{N}^{\pm}$ on $\Gamma_0^{\pm}$ and to solve (BVP1) finally. From now on, we shall assume that the scattering surface Γ is piecewise smooth and satisfies (GC1) only. Though the previous well-posedness theory relies on (GC2), our numerical solver does not rely on such an assumption, and we believe (GC2) can be weakened to at least accept piecewise smooth curves, which we shall investigate in a future work.

6.1 Approximating $\mathcal{N}^{\pm}$

Without loss of generality, consider (BVP2) in an unperturbed cell, say Ω_1^+, and we need to approximate $\mathcal{N}^{(0)}$ first. According to [28], for any $\tilde{u}$ satisfying

$$\nabla \cdot (\mathbf{A}\nabla\tilde{u}) + k^2 \alpha \tilde{u} = 0, \tag{78}$$

on Ω_1^+, we have the following Green's representation theorem

$$\tilde{u}(x) = \int_{\partial\Omega_1^+} \{\tilde{G}(x,y)\partial_{\nu_c}\tilde{u}(y) - \partial_{\nu_c}\tilde{G}(x,y)\tilde{u}(y)\}ds(y), \tag{79}$$

for all $x \in \Omega_1^+$; we recall that ν denotes the outer unit normal vector on $\partial\Omega_1^+$. Moreover, as x approaches $\partial\Omega_1^+ = \cup_{j=1}^4 \overline{\Gamma_{j,1}}$, the usual jump conditions imply [28]

$$\mathcal{K}[\tilde{u}](x) - \mathcal{K}_0[1](x)\tilde{u}(x) = \mathcal{S}\partial_{\nu_c}[\tilde{u}](x), \tag{80}$$

where we have defined the following integral operators

$$\mathcal{S}[\phi](x) = 2\int_{\partial\Omega_1^+} \tilde{G}(x,y)\phi(y)ds(y), \tag{81}$$

$$\mathcal{K}[\phi](x) = 2\text{p.v.}\int_{\partial\Omega_1^+} \partial_{\nu_c}\tilde{G}(x,y)\phi(y)ds(y), \tag{82}$$

$$\mathcal{K}_0[\phi](x) = 2\text{p.v.}\int_{\partial\Omega_1^+} \partial_{\nu_c}\tilde{G}_0(x,y)\phi(y)ds(y), \tag{83}$$

where p.v. indicates the Cauchy principle value, and

$$\tilde{G}_0(x,y) = -\frac{1}{2\pi}\log\rho(\tilde{x},\tilde{y}), \tag{84}$$

is the fundamental solution of the complexified Laplace equation

$$\nabla \cdot (\mathbf{A}\nabla\tilde{u}_0(x)) = 0. \tag{85}$$

Note that theoretically,

$$\mathcal{K}_0[1](x) = -\frac{\theta^{\text{in}}(x)}{\pi}. \tag{86}$$

where $\theta^{\text{in}}(x)$ is defined as the interior angle at x, as indicated in Figure 3(b). However, numerically evaluating $\mathcal{K}_0[1]$ near corners is more advantageous as has been illustrated in the literature [13, 27]. Thus, $\tilde{u} = (\mathcal{K} - \mathcal{K}_0[1])^{-1}\mathcal{S}\partial_{\nu_c}\tilde{u}$ on $\partial\Omega_1^+$. Consequently, the NtD operator $\mathcal{N}_u$ for any unperturbed domain can be defined as

$$\mathcal{N}_u = (\mathcal{K} - \mathcal{K}_0[1])^{-1}\mathcal{S}.$$

To approximate $\mathcal{N}_u$, we need to discretize the three integral operators on the right-hand side. Suppose now the piecewise smooth curve $\partial\Omega_1^+$ is parameterized by $x(s) = \{(x_1(s), x_2(s)) | 0 \le s \le L_1\}$, where s is the arclength parameter. Since corners may exist, $\tilde{u}(x(s))$ can have corner singularities in its derivatives at corners. To smoothen $\tilde{u}$, we introduce a grading function $s = w(t), 0 \le t \le 1$. For a smooth segment of $\partial\Omega_1^+$ corresponding to $s \in [s^0, s^1]$ and $t \in [t^0, t^1]$ such that $s^i = w(t^i)$ for $i = 0, 1$, where s^0 and s^1 correspond to two corners, we take [13, Eq. (3.104)]

$$s = w(t) = \frac{s^0 w_1^p + s^1 w_2^p}{w_1^p + w_2^p}, \quad t \in [t^0, t^1], \tag{87}$$

where the positive integer p ensures that the derivatives of $w(t)$ vanish at the corners up to order p,

$$w_1 = \left(\frac{1}{2} - \frac{1}{p}\right)\xi^3 + \frac{\xi}{p} + \frac{1}{2}, \quad w_2 = 1 - w_1, \quad \xi = \frac{2t - (t^0 + t^1)}{t^1 - t^0}.$$

To simplify notation, we shall use $x(t)$ to denote $x(w(t))$, and $x'(t)$ to denote $\frac{dx}{ds}(w(t))w'(t)$ in the following. Assume that $t \in [0,1]$ is uniformly sampled by an even number, denoted by N, of grid points $\{t_j = jh\}_{j=1}^N$ with grid size $h = 1/N$, and that the grid points contain all the corner points. Thus, $\mathcal{S}[\partial_{\nu_c}\tilde{u}]$ at point $x = x(t_j)$ can be parameterized by

$$\mathcal{S}[\partial_{\nu_c}\tilde{u}](x(t_j)) = \int_0^1 S(t_j, t)\phi^{\mathrm{s}}(t)dt, \tag{88}$$

where $S(t_j, t) = \frac{\mathrm{i}}{2}H_0^{(1)}(k\rho(x(t_j), x(t)))$, and the scaled co-normal vector $\phi^{\mathrm{s}}(t) = \partial_{\nu_c}\tilde{u}(x(t))|x'(t)|$, smoother than $\partial_{\nu_c}\tilde{u}(x(t))$, is introduced to regularize the approximation of $\mathcal{N}_u$.

Considering the logarithmic singularity of $S(t_j, t)$ at $t = t_j$, we can discretize the integral in (88) by Alpert's 6th-order hybrid Gauss-trapezoidal quadrature rule [1] and then by trigonometric interpolation to get

$$\mathcal{S}[\partial_{\nu_c}\tilde{u}^s]\begin{bmatrix} x(t_1) \\ \vdots \\ x(t_N) \end{bmatrix} \approx \mathbf{S}\begin{bmatrix} \phi^{\mathrm{s}}(t_1) \\ \vdots \\ \phi^{\mathrm{s}}(t_N) \end{bmatrix}, \tag{89}$$

where the $N \times N$ matrix $\mathbf{S}$ approximates $\mathcal{S}$. One similarly approximates $\mathcal{K}[\tilde{u}](x(t_j))$ and $\mathcal{K}_0[1](x(t_j))$ for $j = 1, \cdots, N$, so that we obtain, on the boundary of $\partial\Omega_1^+$,

$$\begin{bmatrix} \boldsymbol{u}_{1,1} \\ \boldsymbol{u}_{1,2} \\ \boldsymbol{u}_{1,3} \\ \boldsymbol{u}_{1,4} \end{bmatrix} = \boldsymbol{N}_u \begin{bmatrix} \phi^{\mathrm{s}}_{1,1} \\ \phi^{\mathrm{s}}_{1,2} \\ \phi^{\mathrm{s}}_{1,3} \\ \phi^{\mathrm{s}}_{1,4} \end{bmatrix}, \tag{90}$$

where $\boldsymbol{u}_{1,j'}$ and $\phi^{\mathrm{s}}_{1,j'}$ represent $N_{j'} \times 1$ column vectors of $\tilde{u}$ and ϕ^{s} at the $N_{j'}$ grid points of $\Gamma_{1,j'}$, respectively for $j' = 1, 2, 3, 4$; note that $N = \sum_{j'=1}^4 N_{j'}$ and the grid points on $\Gamma_{1,3}$ are obtained by horizontally translating the grid points on $\Gamma_{1,1}$ so that $N_1 = N_3$. Clearly, the $N \times N$ matrix $\boldsymbol{N}_u$ approximates the scaled NtD operator $\mathcal{N}_u^{\mathrm{s}}$ related to $\mathcal{N}_u$ by $\mathcal{N}_u \partial_{\nu_c}\tilde{u} = \mathcal{N}_u^{\mathrm{s}}\phi^{\mathrm{s}}$. Now, by $\tilde{u}|_{\Gamma_{1,2}\cup\Gamma_{1,4}} = 0$, we eliminate vectors $\boldsymbol{u}_{1,2}$, $\boldsymbol{u}_{1,4}$, $\phi_{1,2}$ and $\phi_{1,4}$ in (90) so that we obtain two $2N_1 \times 2N_1$ matrices $\boldsymbol{N}^{(0)}$ and $\boldsymbol{T}$ that satisfy

$$\begin{bmatrix} \boldsymbol{u}_{1,1} \\ \boldsymbol{u}_{1,3} \end{bmatrix} = \boldsymbol{N}^{(0)}\begin{bmatrix} \phi^{\mathrm{s}}_{1,1} \\ \phi^{\mathrm{s}}_{1,3} \end{bmatrix}, \quad \begin{bmatrix} \phi^{\mathrm{s}}_{1,2} \\ \phi^{\mathrm{s}}_{1,4} \end{bmatrix} = \boldsymbol{T}\begin{bmatrix} \phi^{\mathrm{s}}_{1,1} \\ \phi^{\mathrm{s}}_{1,3} \end{bmatrix}, \tag{91}$$

where we denote

$$\boldsymbol{N}^{(0)} = \left[\begin{array}{cc} \boldsymbol{N}_{00}^{(0)} & \boldsymbol{N}_{01}^{(0)} \\ \boldsymbol{N}_{10}^{(0)} & \boldsymbol{N}_{11}^{(0)} \end{array} \right],$$

with $\boldsymbol{N}_{ij}^{(0)} \in \mathbb{C}^{N_1 \times N_1}$; the above elimination is stable due to the well-posedness of (BVP2) in Theorem 5.1. Note that, different from [28], we no longer simultaneously assume $\tilde{u} = \phi^{\mathrm{s}} = 0$ on $\Gamma_{1,2} \cup \Gamma_{1,4}$, which could cause pronounced error in numerical results. Now compare (60) and (91). Like $\boldsymbol{N}_u$, $\boldsymbol{N}^{(0)}$ approximates the scaled NtD operator $\mathcal{N}^{(0),\mathrm{s}}$ on $\Gamma_1^+ \cup \Gamma_3^+$ related to $\mathcal{N}^{(0)}$ by $\mathcal{N}^{(0)} \partial_{\nu_c} \tilde{u} = \mathcal{N}^{(0),\mathrm{s}} \phi^s$.

Consequently, the previously developed RDP can be easily adapted here in terms of notationally replacing $\mathcal{N}$ by $\boldsymbol{N}$ for the equations (68-77), so that we get two $N_1 \times N_1$ matrices $\boldsymbol{R}_p^+$ and $\boldsymbol{N}^+$ approximating the (scaled) Neumann-marching operator $\mathcal{R}_p^+$ and the (scaled) vNtD operator $\mathcal{N}^+$ such that $\phi_{1,3}^{\mathrm{s}} = -\boldsymbol{R}_p^+ \phi_{1,1}^{\mathrm{s}}$ and $\boldsymbol{u}_{1,1} = \boldsymbol{N}^+ \phi_{1,1}^{\mathrm{s}}$. One similarly obtains two $N_1 \times N_1$ matrices $\boldsymbol{R}_p^-$ and $\boldsymbol{N}^-$ approximating $\mathcal{R}_p^-$ and $\mathcal{N}^-$, respectively.

6.2   Solving (BVP1)

We are now ready to use the PML-based BIE method to solve the main problem (BVP1). For $x^* \in \Omega_0$, to eliminate the δ function, we consider $\tilde{u}^{\mathrm{sc}}(x; x^*) = \tilde{u}^{\mathrm{og}}(x; x^*) - \tilde{u}^{\mathrm{inc}}(x; x^*)$, satisfying (78). For simplicity, we denote (cf. Fig.2 (a))

$$\Gamma_{0,1} = \Gamma_0^-, \quad \Gamma_{0,2} = \Gamma_0, \quad \Gamma_{0,3} = \Gamma_0^+, \quad \text{and} \quad \Gamma_{0,4} = \Gamma_0^{H+L}.$$

Then, analogous to (90), on the four boundaries $\Gamma_{0,j}, j = 1, 2, 3, 4$, we apply the PML-based BIE method in the previous section to approximate the NtD operator for $\tilde{u}^{\mathrm{sc}}$ and $\partial_{\nu_c} \tilde{u}^{\mathrm{sc}}$ on the boundary of the perturbed cell Ω_0 by a matrix $\boldsymbol{N}_p$,

$$\left[\begin{array}{c} \boldsymbol{u}_{0,1}^{\mathrm{sc}} \\ \boldsymbol{u}_{0,2}^{\mathrm{sc}} \\ \boldsymbol{u}_{0,3}^{\mathrm{sc}} \\ \boldsymbol{u}_{0,4}^{\mathrm{sc}} \end{array} \right] = \boldsymbol{N}_p \left[\begin{array}{c} \phi_{0,1}^{\mathrm{sc,s}} \\ \phi_{0,2}^{\mathrm{sc,s}} \\ \phi_{0,3}^{\mathrm{sc,s}} \\ \phi_{0,4}^{\mathrm{sc,s}} \end{array} \right], \tag{92}$$

where $\boldsymbol{u}_{0,j}^{\mathrm{sc}}$ and $\phi_{0,j}^{\mathrm{sc,s}}$ represent column vectors of $\tilde{u}^{\mathrm{sc}}$ and $\partial_{\nu_c} \tilde{u}^{\mathrm{sc}} |x'|$ at the grid points of $\Gamma_{0,j}$, respectively, for $j = 1, 2, 3, 4$. Rewriting the above in terms of $\tilde{u}^{\mathrm{og}}$ and $\partial_{\nu_c} \tilde{u}^{\mathrm{og}}$, we get

$$\left[\begin{array}{c} \boldsymbol{u}_{0,1}^{\mathrm{og}} \\ \boldsymbol{u}_{0,2}^{\mathrm{og}} \\ \boldsymbol{u}_{0,3}^{\mathrm{og}} \\ \boldsymbol{u}_{0,4}^{\mathrm{og}} \end{array} \right] = \boldsymbol{N}_p \left[\begin{array}{c} \phi_{0,1}^{\mathrm{og,s}} \\ \phi_{0,2}^{\mathrm{og,s}} \\ \phi_{0,3}^{\mathrm{og,s}} \\ \phi_{0,4}^{\mathrm{og,s}} \end{array} \right] + \left[\begin{array}{c} \boldsymbol{u}_{0,1}^{\mathrm{inc}} \\ \boldsymbol{u}_{0,2}^{\mathrm{inc}} \\ \boldsymbol{u}_{0,3}^{\mathrm{inc}} \\ \boldsymbol{u}_{0,4}^{\mathrm{inc}} \end{array} \right] - \boldsymbol{N}_p \left[\begin{array}{c} \phi_{0,1}^{\mathrm{inc,s}} \\ \phi_{0,2}^{\mathrm{inc,s}} \\ \phi_{0,3}^{\mathrm{inc,s}} \\ \phi_{0,4}^{\mathrm{inc,s}} \end{array} \right], \tag{93}$$

where $\boldsymbol{u}_{0,j}^{\mathrm{inc}}$ and $\phi_{0,j}^{\mathrm{inc,s}}$ represent column vectors of $\tilde{u}^{\mathrm{inc}}(x; x^*)$ and $\partial_{\nu_c} \tilde{u}^{\mathrm{inc}}(x; x^*)|x'|$ at the grid points of $\Gamma_{0,j}$, respectively, etc.. The boundary conditions in (BVP1) imply that

$$\boldsymbol{u}_{0,2}^{\mathrm{og}} = 0, \quad \boldsymbol{u}_{0,4}^{\mathrm{og}} = 0, \tag{94}$$

$$\boldsymbol{u}_{0,1}^{\mathrm{og}} = \boldsymbol{N}^- \phi_{0,1}^{\mathrm{og,s}}, \quad \boldsymbol{u}_{0,3}^{\mathrm{og}} = \boldsymbol{N}^+ \phi_{0,3}^{\mathrm{og,s}}. \tag{95}$$

Solving the linear system (93-95), we get $\tilde{u}^{\mathrm{og}}(x; x^*)$ and $\partial_{\nu_c} \tilde{u}^{\mathrm{og}}(x; x^*)$ on all grid points of $\partial \Omega_0$.

Now we discuss how to evaluate $\tilde{u}^{\mathrm{og}}(x; x^*)$ in the physical domain S_H. We distinguish two cases:

1. $x \in \Omega_0$. Since on the grid points of $\partial\Omega_0$, $\tilde{u}^{\text{sc}}$ and $\partial_{\nu_c}\tilde{u}^{\text{sc}}|x'|$ are available, we use Green's representation formula (79) with $\partial\Omega_1^+$ replaced by $\partial\Omega_0$ to compute $\tilde{u}^{\text{sc}}(x; x^*)$ in Ω_0 so that $\tilde{u}^{\text{og}}(x; x^*)$ becomes available in Ω_0.

2. $x \in \Omega_j^\pm$. Consider Ω_1^+ first. Suppose $\boldsymbol{u}_{1,j'}^{\text{og}}$ and $\boldsymbol{\phi}_{1,j'}^{\text{og,s}}$ represent column vectors of $\tilde{u}^{\text{og}}$ and $\partial_{\nu_c}\tilde{u}^{\text{og}}|x'|$ at the grid points of $\Gamma_{1,j'}$, for $1 \leq j' \leq 4$. By the continuity of $\partial_{\nu_c}\tilde{u}^{\text{og}}$ on $\Gamma_{1,1} = \Gamma_{0,3} = \Gamma_0^+$, $\boldsymbol{\phi}_{1,1}^{\text{og,s}} = -\boldsymbol{\phi}_{0,3}^{\text{og,s}}$. Since $\boldsymbol{\phi}_{1,3}^{\text{og,s}} = -\boldsymbol{R}_p^+ \boldsymbol{\phi}_{1,1}^{\text{og,s}}$, we get $\boldsymbol{u}_{1,j'}^{\text{og}}$ for $j' = 1, 3$ by (91), and $\boldsymbol{\phi}_{1,j'}^{\text{og,s}}$ for $j' = 2, 4$. Given that $\boldsymbol{u}_{1,2}^{\text{og}} = \boldsymbol{u}_{1,4}^{\text{og}} = 0$, $\tilde{u}^{\text{og}}(x; x^*)$ and $\partial_{\nu_c}\tilde{u}^{\text{og}}|x'|$ on $\partial\Omega_1^+$ become available, so that the Green's representation formula (79) applies to get $\tilde{u}^{\text{og}}(x; x^*)$ in Ω_1^+. Repeating the same procedure, one obtains $\tilde{u}^{\text{og}}(x; x^*)$ in Ω_j^+ for $j \geq 2$. The case for $x \in \Omega_j^-$ can be handled similarly.

Consequently, $u^{\text{tot}}(x; x^*) \approx \tilde{u}^{\text{og}}(x; x^*)$ becomes available for $x \in S_H \subset \overline{\Omega_0} \cup \left[\cup_{j=1}^{\infty} \overline{\Omega_{j,+} \cup \Omega_{j,-}} \right]$.

6.3 Computing u^{tot} for plane-wave incidence

To close this section, we briefly discuss how to compute u^{tot} for a plane incident wave $u^{\text{inc}} = e^{\mathbf{i}k(\cos\theta x_1 - \sin\theta x_2)}$ for $\theta \in (0, \pi)$. First, we consider the non-perturbed case $\Gamma = \Gamma_T$ so that u^{tot} becomes the reference solution $u_{\text{ref}}^{\text{tot}}$. It is clear that $u_{\text{ref}}^{\text{sc}} = u_{\text{ref}}^{\text{tot}} - u^{\text{inc}}$ satisfies the following quasi-periodic condition

$$u_{\text{ref}}^{\text{sc}}(-T/2, x_2) = \gamma u_{\text{ref}}^{\text{sc}}(T/2, x_2), \tag{96}$$

$$\partial_{x_1} u_{\text{ref}}^{\text{sc}}(-T/2, x_2) = \gamma \partial_{x_1} u_{\text{ref}}^{\text{sc}}(T/2, x_2), \tag{97}$$

where $\gamma = e^{\mathbf{i}k\cos\theta T}$. On Γ, we have from (2) that

$$u_{\text{ref}}^{\text{sc}} = -u^{\text{inc}}. \tag{98}$$

Due to the quasi-periodicity, above $x_2 = H$, we could express $u_{\text{ref}}^{\text{sc}}$ in terms of a Fourier series, i.e.,

$$u_{\text{ref}}^{\text{sc}}(x_1, x_2) = \sum_{j=-\infty}^{\infty} R_j e^{\mathbf{i}\alpha_j x_1 + \mathbf{i}\beta_j x_2}, \quad x_2 \geq H, \tag{99}$$

where $\alpha_j = k\cos\theta + \frac{2\pi j}{T}$ and $\beta_j = \sqrt{k^2 - \alpha_j^2}$ if $|\alpha_j| \leq k$, otherwise $\beta_j = \mathbf{i}\sqrt{\alpha_j^2 - k^2}$, and R_j denotes the j-th reflective coefficient. Thus, the complexified field $\tilde{u}_{\text{ref}}^{\text{sc}}(x_1, x_2) = u_{\text{ref}}^{\text{sc}}(x_1, \tilde{x}_2)$ satisfies on the PML boundary $x_2 = L + H$

$$\tilde{u}_{\text{ref}}^{\text{sc}}(x_1, L + H) = \sum_{j=-\infty}^{\infty} R_j e^{\mathbf{i}\alpha_j x_1 + \mathbf{i}\beta_j(H+L) - \beta_j S_c L}. \tag{100}$$

For simplicity, we assume that all β_j are sufficiently away from 0, so that provided that L and S_c are sufficiently large, we can directly impose the following Dirichlet boundary condition

$$\tilde{u}_{\text{ref}}^{\text{sc}}(x_1, H + L) = 0. \tag{101}$$

If β_j is quite close to 0, accurate boundary conditions can be developed; we refer readers to [26, 29, 34] for details. Besides, $\tilde{u}_{\text{ref}}^{\text{sc}}$ satisfies the quasi-periodic conditions (96) and (97) and the surface condition (98), but with u replaced by $\tilde{u}$.

On the boundary $\partial\Omega_0$, the PML-BIE method gives, analogous to (92),

$$\begin{bmatrix} \boldsymbol{u}_1^{\mathrm{sc}} \\ \boldsymbol{u}_2^{\mathrm{sc}} \\ \boldsymbol{u}_3^{\mathrm{sc}} \\ \boldsymbol{u}_4^{\mathrm{sc}} \end{bmatrix} = \boldsymbol{N}_p \begin{bmatrix} \boldsymbol{\phi}_1^{\mathrm{sc}} \\ \boldsymbol{\phi}_2^{\mathrm{sc}} \\ \boldsymbol{\phi}_3^{\mathrm{sc}} \\ \boldsymbol{\phi}_4^{\mathrm{sc}} \end{bmatrix}, \tag{102}$$

where $\boldsymbol{u}_{j'}^{\mathrm{sc}}$ and $\boldsymbol{\phi}_{j'}^{\mathrm{sc}}$ represent vectors of $\tilde{u}_{\mathrm{ref}}^{\mathrm{sc}}$ and $\partial_{\nu_c}\tilde{u}_{\mathrm{ref}}^{\mathrm{sc}}|w'|$ at the grid points of $\Gamma_{0,j'}$, respectively, for $1 \le j' \le 4$; note that $\boldsymbol{N}_p$ is the same as $\boldsymbol{N}_u$ in (90) since $\Gamma = \Gamma_T$. Equation (101) directly implies that

$$\boldsymbol{u}_4^{\mathrm{sc}} = 0. \tag{103}$$

The quasi-periodic conditions (96) and (97) imply

$$\boldsymbol{u}_3^{\mathrm{sc}} = \gamma\boldsymbol{u}_1^{\mathrm{sc}}, \quad \boldsymbol{\phi}_3^{\mathrm{sc}} = -\gamma\boldsymbol{\phi}_1^{\mathrm{sc}}. \tag{104}$$

The interface condition (98) indicates

$$\boldsymbol{u}_2^{\mathrm{sc}} = -\boldsymbol{u}_2^{\mathrm{inc}}, \tag{105}$$

where $\boldsymbol{u}_2^{\mathrm{inc}}$ represents the vector of u^{inc} at grid points of $\Gamma_{0,2}$. Solving the linear system (102-105) gives rise to values of $\tilde{u}_{\mathrm{ref}}^{\mathrm{sc}}$ and $\partial_{\nu_c}\tilde{u}_{\mathrm{ref}}^{\mathrm{sc}}|w'|$ on $\partial\Omega_0$. The Green's representation formula (79) can help to compute $\tilde{u}_{\mathrm{ref}}^{\mathrm{sc}}$ in Ω_0. The quasi-periodicity helps to construct $\tilde{u}_{\mathrm{ref}}^{\mathrm{sc}}$ in any other cells $\Omega_j^{\pm}$ for $j \in \mathbb{N}^*$. Consequently, $u_{\mathrm{ref}}^{\mathrm{tot}}$ becomes available in the physical domain S_H.

Now, if Γ is a local perturbation of Γ_T, as $\tilde{u}_{\mathrm{ref}}^{\mathrm{sc}}$ is available now, one follows the same approach developed in section 6.2 to get $\tilde{u}^{\mathrm{og}} = \tilde{u}^{\mathrm{sc}} - \tilde{u}_{\mathrm{ref}}^{\mathrm{sc}}$ in any unperturbed cell and thus u^{tot} in the physical region S_H. We omit the details here.

7 Numerical examples

In this section, we will carry out four numerical experiments to validate the performance of the PML-based BIE method and also the proposed theory. In all examples, we set the free-space wavelength $\lambda = 1$ so that $k_0 = 2\pi$, and the period $T = 1$. We consider two types of incidence: (1) a cylindrical incidence excited by source point $x^* = (0, 1.5)$; (2) a plane-wave incidence of angle θ to be specified. We suppose that only one unit cell of the background periodic structure is perturbed. To setup the PML, we let $m = 0$ in (17) to define σ for simplicity. In the RDP iterations (73), (74), (76) and (77), we take $l = 20$. Furthermore, we choose $H = 3$ and set the computational domain to be $[-5.5, 5.5] \times [-2, 3]$, which contains 11 cells. To validate the accuracy of our method, we compute the relative error

$$E_{\mathrm{rel}} := \frac{||(\boldsymbol{\phi}_{2,0}^{\mathrm{sc,s}})^{\mathrm{num}} - (\boldsymbol{\phi}_{2,0}^{\mathrm{sc,s}})^{\mathrm{exa}}||_{\infty}}{||(\boldsymbol{\phi}_{2,0}^{\mathrm{sc,s}})^{\mathrm{exa}}||_{\infty}},$$

for $\boldsymbol{\phi}_{2,0}^{\mathrm{sc,s}}$ representing the scaled normal derivative $|w'|\partial_{\nu}u^{\mathrm{sc}}$ on $\Gamma_{2,0}$, the perturbed part of Γ, and for different values of S and L in the setup of the PML, where superscript "num" indicates numerical solution, superscript "exa" indicates a sufficiently accurate numerical solution or the exact solution if available.

Example 1: a flat curve. In the first example, we assume that Γ is the straight line $\{x : x_2 = 0\}$. Certainly, we can regard such a simple structure as a periodic structure

with period equal to one wavelength. We regard the line segment between $x_1 = -0.5$ and $x_1 = 0.5$ on Γ as segment $\Gamma_{0,2}$, i.e., as the "perturbed" part. For the cylindrical incidence, the total wave field u^{tot} is given by

$$u^{\mathrm{tot}}(x; x^*) = \frac{\mathbf{i}}{4}\left[H_0^{(1)}(k|x - x^*|) - H_0^{(1)}(k|x - x^*_{\mathrm{imag}}|)\right],$$

where the image source point $x^*_{\mathrm{imag}} = (0, -1.5)$. Using this to compute the scaled co-normal derivative on segment $\Gamma_{0,2}$, we get the reference solution and can check the accuracy of our method. We discretize each smooth segment of the perturbed/unperturbed unit cell by 600 grid points. To check how the wavenumber condition in Theorem 5.1 affect the accuracy of our numerical solver, we consider two values of the refractive index n in Ω: (1) $n = 1.03$ so that $kT/\pi = 2.06 \notin \mathcal{E}$; (2) $n = 1$ so that $kT/\pi = 2 \in \mathcal{E}$. For both cases, we compare results of Dirichlet and Neumann boundary conditions on Γ_{H+L}.

For $n = 1.03$, Figure 4 (a) and (b) compare the exact solution and our numerical solution for $L = 2.2$ and $S = 2.8$. The two solutions are indistinguishable. To give a

(a)   (b)   (c)   (d)
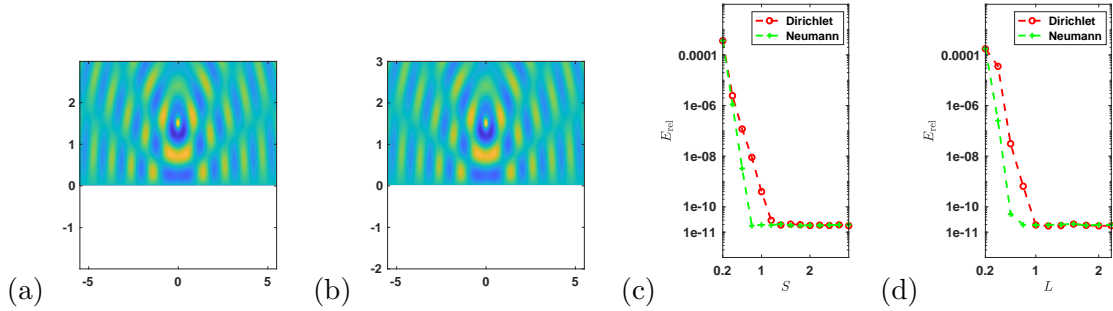
Figure 4: Example 1: Real part of u^{tot} in $[-5.5, 5.5] \times [-2.0, 3.0]$ excited by the point source $y = (0, 1.5)$: (a) exact solution; (b) numerical solution. Convergence history of relative error E_{rel} versus: (c) PML absorbing constant S; (d) Thickness of the PML L, for both Dirichlet and Neumann conditions on Γ_{H+L}.

detailed comparison, Figure 4 (c) and (d) show how the relative error E_{rel} decays as one of the two PML parameters, the absorbing constant S and the thickness L, increases for either zero Dirichlet or zero Neumann condition on Γ_{H+L}. In Figure 4(c), we take $L = 2.2$ and let S vary between 0.2 and 2.8, while in Figure 4(d), we take $S = 2.8$ and let the PML thickness L vary between 0.2 and 2.2. In both figures, the vertical axis is logarithmically scaled so that the vertical dashed lines indicate that the relative error E_{rel} decays exponentially as L or S increases for both conditions. On the other hand, Neumann condition gives faster convergence rate than Dirichlet condition. The convergence curves indicate nearly 11 significant digits are revealed by the proposed PML-based BIE method. The 'o' lines in Figure 5(a) show the convergence curve of

$$E_{\mathrm{Ric}} = ||\boldsymbol{N}_{10}^{(0)} + [\boldsymbol{N}_{11}^{(0)} + \boldsymbol{N}_{00}^{(0)}]\boldsymbol{R}_p^+ + \boldsymbol{N}_{01}^{(0)}(\boldsymbol{R}_p^+)^2||_\infty \tag{106}$$

against the number of iterations l. It can be seen that after only 11 iterations, $\boldsymbol{R}_p^+$ satisfies its governing Riccati equation (62) up to round-off errors. The 'o' lines in Figure 5(b) show the curve of $||\phi^{\mathrm{og,s}}|_{\Gamma_j^+}||_\infty$ against j. It can be seen that $\phi^{\mathrm{og,s}}$ and hence $\partial_{\nu_c^+} u^{\mathrm{og}}$ indeed decay exponentially as j or x_1 increases, as has been illustrated in Corollary 5.1.

In Figure 5(c), we compare Dirichlet and Neumann conditions for $n = 1$. We take $L = 2.2$ and let S vary from 0.2 to 2.8. Among the four convergence curves, solid lines indicate

(a)　　　　　　　　　(b)　　　　　　　　　(c)
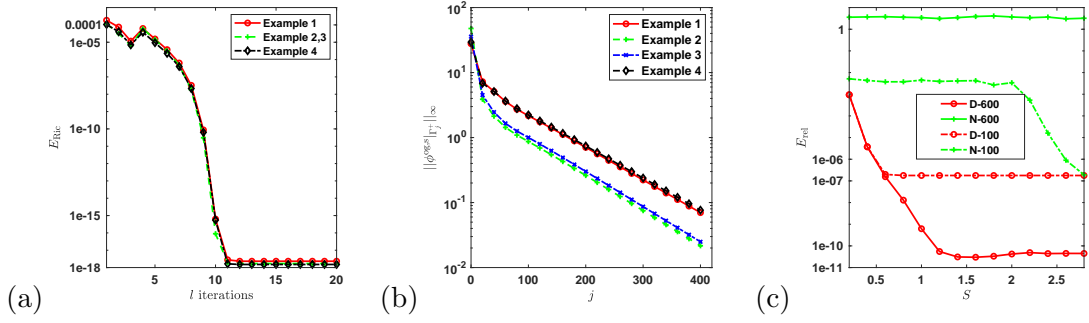
Figure 5: All four examples: (a) Convergence history of E_{Ric} in (106) against the number of iterations l; (b) Radiation behavior of $\phi^{\mathrm{og,s}}|_{\Gamma_j^+}$ as $j \to \infty$. (c): Performance of Dirichlet and Neumann conditions in Example 1 for $n = 1$, at which $kT/\pi \in \mathbb{Q}^+$; here 'D' stands for Dirichlet and 'N' for Neumann, and 100 indicates 100 grid points are used to discretize each smooth segment of the unit cells, etc..

600 grid points chosen on each smooth segment of each unit cell, while dashed lines indicate 100 grid points; '+' indicates Neumann condition on Γ_{H+L} while 'o' indicates Dirichlet condition. If 100 grid points are used, E_{rel} for Neumann condition starts decreasing after $S \geq 2$ whereas E_{rel} for Dirichlet condition has already reached its minimum error; if 600 grid points are used, Neumann condition does not make E_{rel} converge at all for $S \in [0.2, 2.8]$, but Dirichlet condition still possesses the same convergence rate and accuracy as in case $n = 1.03$. Consequently, Dirichlet condition outperforms Neumann condition for $n = 1$.

Example 2: a sine curve. In the second example, we assume that Γ is the sine curve, $x_2 = \sin(2\pi x_1 + \pi)$, as shown in Figure 6(a) and that $n = 1.03$ to make $kT/\pi \notin \mathbb{Q}^+$. For the

(a)　　　　　　　　　(b)　　　　　　　　　(c)
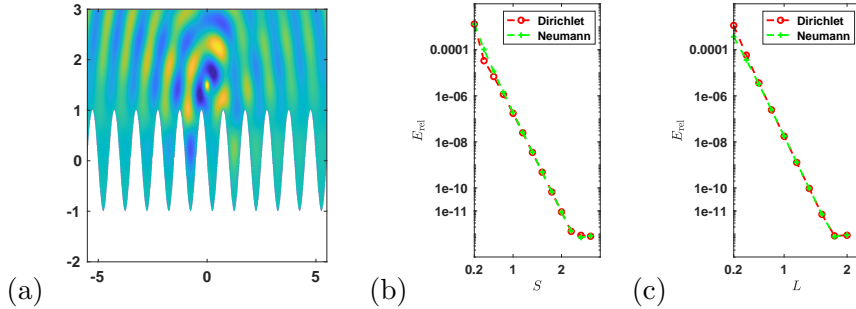
Figure 6: Example 2: (a) Numerical solution of real part of the total wave field u in $[-5.5, 5.5] \times [-2.0, 3.0]$ excited by the point source $y = (0, 1.5)$. Convergence history of relative error E_{rel} versus: (b) PML absorbing constant S for fixed PML Thickness $L = 2$, (c) PML Thickness L for fixed PML absorbing constant $S = 2.8$; vertical axes are logarithmically scaled.

cylindrical incidence, we discretize each smooth segment of any unit cell by 600 grid points, and compare results of Dirichlet and Neumann boundary conditions on Γ_{H+L}. Taking $S = 2.8$ and $L = 2.2$, we evaluate the wave field in $[-5.5, 5.5] \times [-2.0, 3.0]$ and use this as the reference solution since the exact solution is no longer available. In Figure 6, (a) shows the field pattern of the reference solution, and (b) and (c) show the convergence history of relative error E_{rel} versus one of the two PML parameters S and L, respectively. Again,

we observe that E_{rel} decays exponentially as S or L increases. Unlike the flat surface in Example 1, we no longer observe a faster convergence rate of Neumann condition, but find that both conditions share the same convergence rate and accuracy. Considering its worse result for $kT/\pi \in \mathbb{Q}$ and unimpressive improvement for $kT/\pi \notin \mathbb{Q}$, we conclude that Neumann condition is less superior than Dirichlet condition, and thus shall only use the latter one in the rest experiments. With Dirichlet condition, the '+' lines in Figure 5 (a) show the convergence curve of E_{Ric} in (106) against the number of iterations l. The '+' lines in Figure 5 (b) show the curve of $||\phi^{\text{og,s}}|_{\Gamma_j^+}||_\infty$ against j.

For the plane-wave incidence, we take $\theta = \frac{\pi}{3}$. Employing the method in section 6.3, we discretize each smooth segment of any unit cell by 700 grid points. Taking $S = 2.8$ and $L = 4$, we evaluate the wave field in $[-5.5, 5.5] \times [-2.0, 3.0]$ and use this as the reference solution. In Figure 7, (a) shows the field pattern, and (b) and (c) show the

(a) (b) (c)
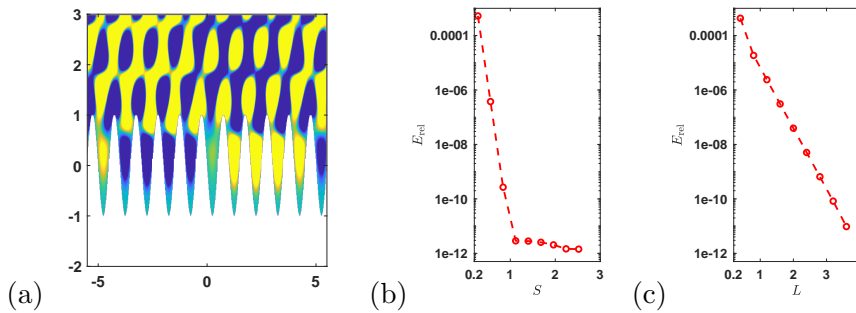
Figure 7: Example 2: (a) Numerical solution of real part of the total wave field u in $[-5.5, 5.5] \times [-2.0, 3.0]$ excited by a plane incident wave of angle $\theta = \frac{\pi}{3}$. Convergence history of relative error E_{rel} versus: (b) PML absorbing constant S for fixed PML Thickness $L = 4$, (c) PML Thickness L for fixed PML absorbing constant $S = 2.8$; vertical axes are logarithmically scaled.

convergence history of relative error E_{rel} versus one of the two PML parameters S and L, respectively. For both incidences, the convergence curves in Figures 6 and 7 decay exponentially, indicating that nearly 12 significant digits are revealed by the proposed PML-based BIE method.

Example 3: a locally perturbed sine curve. In the third example, we assume that the sine curve $\Gamma : x_2 = \sin(2\pi x_1 + \pi)$ is locally perturbed with the part between $x_1 = -0.5$ and $x_1 = 0.5$ replaced by the line segment $\{(x_1, 0) : x_1 \in [-0.5, 0.5]\}$, as shown in Figure 8 (a). For the cylindrical incidence, we discretize each smooth segment of any unit cell by 600 grid points. Taking $S = 2.8$ and $L = 2.2$, we evaluate the wave field in $[-5.5, 5.5] \times [-2.0, 3.0]$ and use this as the reference solution, the field pattern of which is shown in Figure 8 (a). The 'x' lines in Figure 5 (b) show the curve of $||\phi^{\text{og,s}}|_{\Gamma_j^+}||_\infty$ against j.

For the plane incidence, we take $\theta = \frac{\pi}{3}$ and discretize each smooth segment of any unit cell by 700 grid points. Taking $S = 2.8$ and $L = 4$, we evaluate the wave field in $[-5.5, 5.5] \times [-2.0, 3.0]$ and use this as the reference solution, the field pattern of which is shown in Figure 8 (b).

For both incidences, Figure 8 (c) and (d) show the convergence history of relative error E_{rel} versus one of the two PML parameters S and L, respectively. The convergence curves decay exponentially and indicate that nearly 11 significant digits are revealed by the proposed PML-based BIE method.
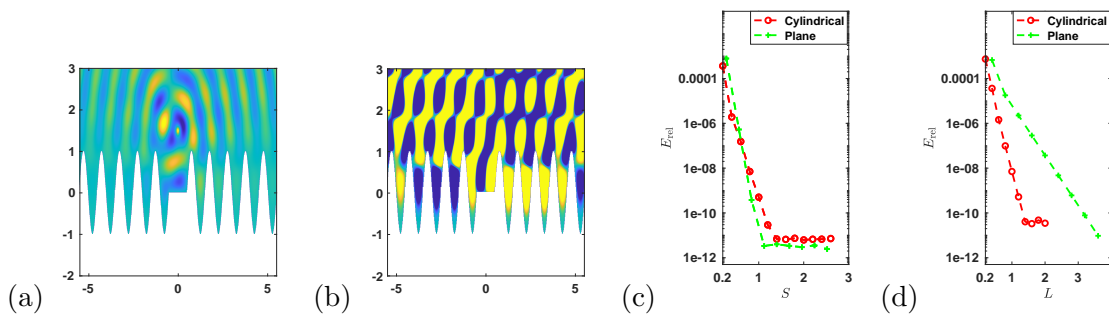
Figure 8: Example 3: Numerical solution of real part of the total wave field u in $[-5.5, 5.5] \times [-2.0, 3.0]$ excited by: (a) a cylindrical wave by source $y = (0, 1.5)$; (b) a plane wave of incident angle $\theta = \frac{\pi}{3}$. Convergence history of relative error E_{rel} versus: (c) PML Thickness L for fixed PML absorbing constant $S = 2.8$ for both incidences; (d) PML absorbing constant S for fixed PML Thickness $L = 2.2$ (4.0) for cylindrical (plane-wave) incidence.

Example 4: a locally perturbed binary grating. In the last example, we assume that Γ consists of periodic rectangular grooves of depth 0.5 and width 0.25, with the part between $x_1 = -0.5$ and $x_1 = 0.5$ replaced by the line segment $\{(x_1, 0) : x_1 \in [-0.5, 0.5]\}$, as shown in Figure 9(a). For the cylindrical incidence, we discretize each smooth segment of
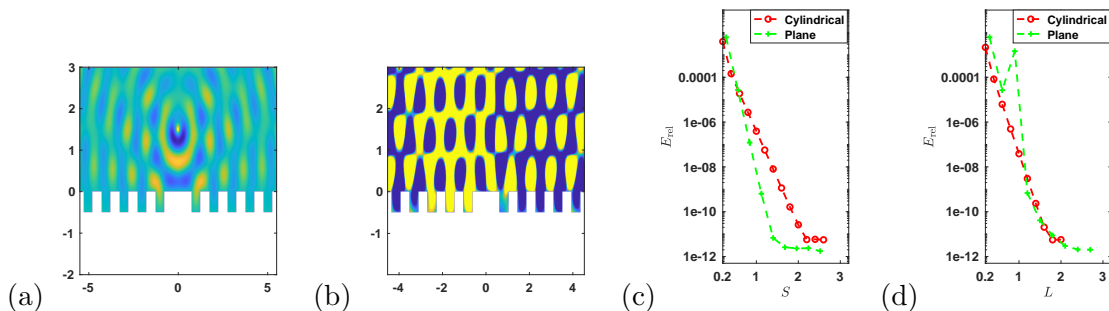
Figure 9: Example 4: Numerical solution of real part of the total wave field u in $[-5.5, 5.5] \times [-2.0, 3.0]$ excited by: (a) a cylindrical wave by source $y = (0, 1.5)$; (b) a plane wave of incident angle $\theta = \frac{\pi}{6}$. Convergence history of relative error E_{rel} versus: (c) PML Thickness L for fixed PML absorbing constant $S = 2.8$ for both incidences; (d) PML absorbing constant S for fixed PML Thickness $L = 2.2$ (3.0) for cylindrical (plane-wave) incidence.

any unit cell by 600 grid points. Taking $S = 2.8$ and $L = 2.2$, we evaluate the wave field in $[-5.5, 5.5] \times [-2.0, 3.0]$ and use this as the reference solution, the field pattern of which is shown in Figure 9 (a). The '$\diamondsuit$' lines in Figure 5 (a) show the convergence curve of E_{Ric} in (106) against the number of iterations l. The '$\diamondsuit$' lines in Figure 5 (b) show the curve of $||\phi^{\text{og,s}}|_{\Gamma_j^+}||_\infty$ against j.

For the plane-wave incidence, we take $\theta = \frac{\pi}{6}$ and discretize each smooth segment of any unit cell by 600 grid points. Taking $S = 2.8$ and $L = 3$, we evaluate the wave field in $[-5.5, 5.5] \times [-2.0, 3.0]$ and use this as the reference solution, the field pattern of which is shown in Figure 9 (b).

For both incidences, Figure 9 (c) and (d) show the convergence history of relative error E_{rel} versus one of the two PML parameters S and L, respectively. The convergence

curves decay exponentially and indicate that nearly 12 significant digits are revealed by the proposed PML-based BIE method.

8 Conclusion

This paper studied the perfectly-matched-layer (PML) theory for wave scattering in a half space of homogeneous medium bounded by a two-dimensional, perfectly conducting, and locally defected periodic surface, and developed a high-accuracy boundary-integral-equation (BIE) solver. By placing a PML in the vertical direction to truncate the unbounded domain to a strip, we proved that the PML solution converges to the true solution in the physical subregion of the strip at an algebraic order of the PML thickness. Laterally, the unbounded strip is divided into three regions: a region containing the defect and two semi-waveguide regions of periodic subsurfaces, separated by two vertical line segments. We proved the well-posedness of an associated scattering problem in both semi-waveguide so as to well define a Neumann-to-Dirichlet (NtD) operator on the associated vertical segment. The two NtD operators, serving as exact lateral boundary conditions, reformulate the unbounded strip problem as a boundary value problem over the defected region. Each NtD operator is closely related to a Neumann-marching operator, governed by a nonlinear Riccati equation, which was efficiently solved by an RDP method and a high-accuracy PML-based BIE method so that the boundary value problem on the defected region can be solved finally. Our future research plan shall focus on the following two aspects:

(1). Extend the current work to study locally defected periodic structures of stratified media. In such case, propagating Bloch modes may exist so that the related Neumann marching operators $\mathcal{R}_p^\pm$ may not be contracting.

(2). Rigorously justify that the PML solution converges exponentially to the true solution in any compact subset of the strip, as has been demonstrated by numerical experiments.

References

[1] B. K. Alpert. Hybrid Gauss-trapezoidal quadrature rules. *SIAM Journal on Scientific Computing*, 20(5):1551–1584, 1999.

[2] T. Arens and T. Hohage. On radiation conditions for rough surface scattering problems. *IMA Journal of Applied Mathematics*, 70(6):839–847, 2005.

[3] G. Bao, D. C. Dobson, and J. A. Cox. Mathematical studies in rigorous grating theory. *J. Opt. Soc. Am. A*, 12(5):1029–1042, 1995.

[4] J.-P. Berenger. A perfectly matched layer for the absorption of electromagnetic waves. *J. Comput. Phys.*, 114(2):185 – 200, 1994.

[5] S. N. Chandler-Wilde and J. Elschner. Variational approach in weighted sobolev spaces to scattering by unbounded rough surfaces. *SIAM J. Math. Analy.*, 42, 2010.

[6] S. N. Chandler-Wilde and P. Monk. The pml for rough surface scattering. *Applied Numerical Mathematics*, 59:2131–2154, 2009.

[7] S. N. Chandler-Wilde and P. Monk. Existence, uniqueness and variational methods for scattering by unbounded rough surfaces. *SIAM J. Math. Analy.*, 37, 2015.

[8] S. N. Chandler-Wilde, C. R. Ross, and B. Zhang. Scattering by infinite one-dimensional rough surfaces. *Proc. R. Soc. Lon. A*, 455:3767–3787, 1999.

[9] S. N. Chandler-Wilde and B. Zhang. Electromagnetic scattering by an inhomogeneous conducting or dielectric layer on a perfectly conducting plate. *Proc. Roy. Soc. London A*, 454:519–542, 1998.

[10] Z. Chen and H. Wu. An adaptive finite element method with perfectly matched absorbing layers for the wave scattering by periodic structures. *SIAM J. Numer. Analy.*, 41(3):799–826, 2003.

[11] W. C. Chew. *Waves and fields in inhomogeneous media*. IEEE PRESS, New York, 1995.

[12] W. C. Chew and W. H. Weedon. A 3D perfectly matched medium for modified Maxwell's equations with stretched coordinates. *Microwave and Optical Technology Letters*, 7(13):599–604, 1994.

[13] D. Colton and R. Kress. *Inverse Acoustic and Electromagnetic Scattering Theory (3rd Edition)*. Springer, 2013.

[14] J. A. DeSanto and P. A. Martin. On angular-spectrum representations for scattering by infinite rough surfaces. *Wave Motion*, 24:421–433, 1996.

[15] M. Ehrhardt, H. Han, and C. Zheng. Numerical simulation of waves in periodic structures. *Commun. in Comp. Phys.*, 5(5):849–870, 2009.

[16] A. Fichtner. *Full Seismic Waveform Modelling and Inversion*. Springer, 2011.

[17] S. F. Helfert and R. Pregla. Efficient analysis of periodic structure. *J. Lightwave Technol.*, 16:1694–1702, 1998.

[18] G. Hu, W. Lu, and A. Rathsfeld. Time-harmonic acoustic scattering from locally perturbed periodic curves. *submitted*, 2020.

[19] Z. Hu and Y. Y. Lu. Efficient numerical method for analyzing coupling structures of photonic crystal waveguides. *IEEE Photon. Tech. Lett.*, 21(23):1737–1739, 2009.

[20] S. Johnson. Notes on Perfectly Matched Layers (PMLs), http://www-math.mit.edu/ stevenj/18.369/spring09/pml.pdf. *Unpublished*, 2008.

[21] P. Joly, J-R. Li, and S. Fliss. Exact boundary conditions for periodic waveguides containing a local perturbation. *Commun. in Comp. Phys.*, 1(6):945–973, 2006.

[22] T. Kato. *Perturbation Theory for Linear Operators*. Classics in Mathematics, SpringerVerlag, Berlin,, 1995, Reprint of the 1980 edition.

[23] M. Lassas and E. Somersalo. Analysis of the PML equations in general convex geometry. *Proceedings of the Royal Society of Edinburgh: Section A Mathematics*, 131(5):1183–1207, 2001.

[24] A. Lechleiter and R. Zhang. A Floquet-Bloch transform based numerical method for scattering from locally perturbed periodic surfaces. *SIAM J. Sci. Comput.*, 39(5):B819–B839, 2017.

[25] W. Lu. Mathematical analysis of wave radiation by a step-like surface. *SIAM J. Appl. Math.*, 81(2):666–693, 2021.

[26] W. Lu and Y. Y. Lu. High order integral equation method for diffraction gratings. *J. Opt. Soc. Am. A*, 29(5):734–740, 2012.

[27] W. Lu and Y. Y. Lu. Efficient high order waveguide mode solvers based on boundary integral equations. *J. Comput. Phys.*, 272:507 – 525, 2014.

[28] W. Lu, Y. Y. Lu, and J. Qian. Perfectly matched layer boundary integral equation method for wave scattering in a layered medium. *SIAM J. Appl. Math.*, 78(1):246–265, 2018.

[29] W. Lu, Y. Y. Lu, and D. Song. A numerical mode matching method for wave scattering in a layered medium with a stratified inhomogeneity. *SIAM J. Sci. Comput.*, 41(2):B274–B294, 2019.

[30] W. McLean. *Strongly Elliptic Systems and Boundary Integral Equations*. Cambridge University Press, New York, NY, 2000.

[31] P. Monk. *Finite Element Methods for Maxwell's Equations*. Oxford University Press, 2003.

[32] J. Sun and C. Zheng. Numerical scattering analysis of te plane waves by a metallic diffraction grating with local defects. *J. Opt. Soc. Am. A*, 26(1):156–162, 2009.

[33] L. Yuan and Y. Y. Lu. A recursive doubling dirichlet-to-neumann map method for periodic waveguides. *J. Lightwave Technol.*, 25:3649–3656, 2007.

[34] W. Zhou and H. Wu. An adaptive finite element method for the diffraction grating problem with PML and few-mode dtn truncations. *J. Sci. Comput.*, 76:1813–1838, 2018.